PSMD11 loss-of-function variants correlate with a neurobehavioral phenotype, obesity, and increased interferon response

Graphical abstract

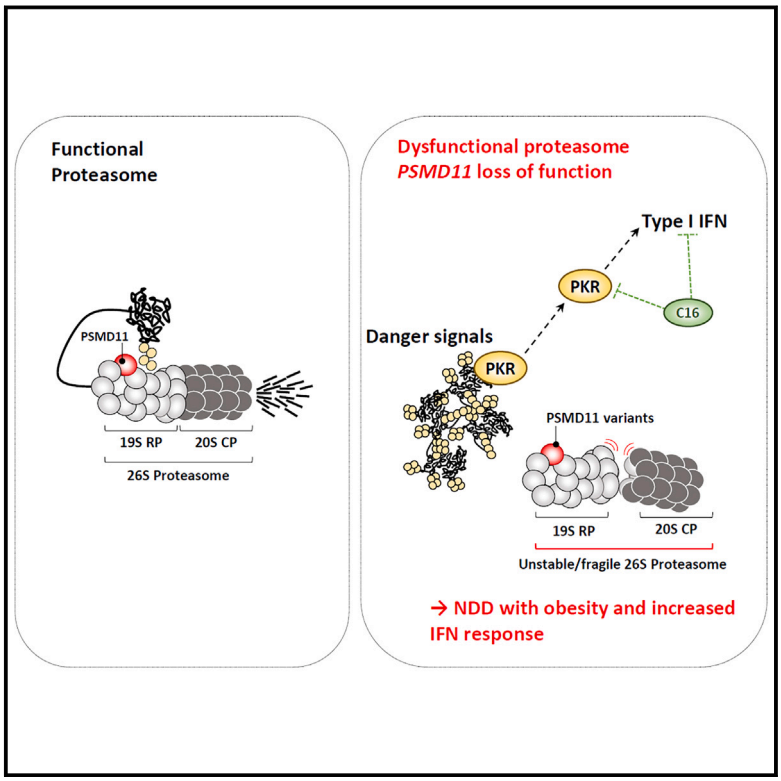

Authors

Wallid Deb, Cory Rosenfelt, Virginie Vignard, ..., Elke Krüger, Sébastien Küry, Frédéric Ebstein

Correspondence

elke.krueger@uni-greifswald.de (E.K.), frederic.ebstein@univ-nantes.fr (F.E.)

Deb et al. have identified *PSMD11*, which encodes a proteasome subunit, as a causative factor for a neurodevelopmental disorder. Their investigations involving clinical phenotype analysis and proband-derived cell lines as well as animal and cellular models have established an association between *PSMD11* variants and impaired learning abilities, obesity, and auto-inflammation.

Deb et al., 2024, The American Journal of Human Genetics *111*, 1352–1369
July 11, 2024
https://doi.org/10.1016/j.ajhg.2024.05.016

ARTICLE

PSMD11 loss-of-function variants correlate with a neurobehavioral phenotype, obesity, and increased interferon response

Wallid Deb,[1,2] Cory Rosenfelt,[3] Virginie Vignard,[1,2] Jonas Johannes Papendorf,[4] Sophie Möller,[4] Martin Wendlandt,[4] Maja Studencka-Turski,[4] Benjamin Cogné,[1,2] Thomas Besnard,[1,2] Léa Ruffier,[2] Bérénice Toutain,[2] Léa Poirier,[2] Silvestre Cuinat,[1,2] Amy Kritzer,[5,6] Amy Crunk,[7] Janette diMonda,[8] Jaime Vengoechea,[8] Sandra Mercier,[1,2] Lotte Kleinendorst,[9,10] Mieke M. van Haelst,[9,10,11] Linda Zuurbier,[9,11] Telma Sulem,[12] Hildigunnur Katrínardóttir,[12] Rún Friðriksdóttir,[12] Patrick Sulem,[12] Kari Stefansson,[12] Berglind Jonsdottir,[13] Shimriet Zeidler,[14] Margje Sinnema,[15] Alexander P.A. Stegmann,[15] Natali Naveh,[16] Cara M. Skraban,[16,17,18] Christopher Gray,[16,17] Jill R. Murrell,[19] Sedat Isikay,[20] Davut Pehlivan,[21,22,23] Daniel G. Calame,[21,22,23] Jennifer E. Posey,[21] Mathilde Nizon,[1,2] Kirsty McWalter,[7] James R. Lupski,[21,23,24,25] Bertrand Isidor,[1,2] François V. Bolduc,[3,26,27] Stéphane Bézieau,[1,2,28] Elke Krüger,[4,28,*] Sébastien Küry,[1,2,28] and Frédéric Ebstein[2,4,28,*]

Summary

Primary proteasomopathies have recently emerged as a new class of rare early-onset neurodevelopmental disorders (NDDs) caused by pathogenic variants in the *PSMB1*, *PSMC1*, *PSMC3*, or *PSMD12* proteasome genes. Proteasomes are large multi-subunit protein complexes that maintain cellular protein homeostasis by clearing ubiquitin-tagged damaged, misfolded, or unnecessary proteins. In this study, we have identified *PSMD11* as an additional proteasome gene in which pathogenic variation is associated with an NDD-causing proteasomopathy. *PSMD11* loss-of-function variants caused early-onset syndromic intellectual disability and neurodevelopmental delay with recurrent obesity in 10 unrelated children. Our findings demonstrate that the cognitive impairment observed in these individuals could be recapitulated in *Drosophila melanogaster* with depletion of the *PMSD11* ortholog *Rpn6*, which compromised reversal learning. Our investigations in subject samples further revealed that *PSMD11* loss of function resulted in impaired 26S proteasome assembly and the acquisition of a persistent type I interferon (IFN) gene signature, mediated by the integrated stress response (ISR) protein kinase R (PKR). In summary, these data identify *PSMD11* as an additional member of the growing family of genes associated with neurodevelopmental proteasomopathies and provide insights into proteasomal biology in human health.

Introduction

Since their initial characterization in the 1980s,[1–3] proteasomes have been the focus of intense investigations across a wide range of research domains. Their remarkable capacity to swiftly eliminate protein substrates tagged with ubiquitin chains as degradation signals makes them essential to the regulation of nearly all fundamental cellular processes.[4] As ubiquitination may selectively target virtually all proteins in response to damage, misfolding, or physiological stimuli, proteasomes are indeed involved in a vast array of processes that include protein quality control, gene expression, signal transduction, and major histocompatibility complex (MHC) class I antigen presentation.[5]

[1]Nantes Université, CHU Nantes, Service de Génétique Médicale, 44000 Nantes, France; [2]Nantes Université, CNRS, INSERM, l'institut du thorax, 44000 Nantes, France; [3]Department of Pediatrics, University of Alberta, Edmonton, AB T6G 1C9, Canada; [4]Institut für Medizinische Biochemie und Molekularbiologie (IMBM), Universitätsmedizin Greifswald, Ferdinand-Sauerbruch-Straße, 17475 Greifswald, Germany; [5]Division of Genetics and Genomics, Department of Medicine, Boston Children's Hospital, Boston, MA 02115, USA; [6]Harvard Medical School, Boston, MA, USA; [7]GeneDx, Gaithersburg, MD 20877, USA; [8]Department of Human Genetics, School of Medicine, Emory University, Atlanta, GA, USA; [9]Amsterdam Reproduction & Development Research Institute, Amsterdam UMC, University of Amsterdam, Amsterdam, the Netherlands; [10]Emma Center for Personalized Medicine, Amsterdam UMC, University of Amsterdam, Amsterdam, the Netherlands; [11]Department of Human Genetics, Amsterdam UMC, Amsterdam UMC, Location AMC, Amsterdam, the Netherlands; [12]deCODE Genetics/Amgen, Inc., Reykjavik, Iceland; [13]Childrens Hospital Hringurinn, National University Hospital of Iceland, Reykjavik, Iceland; [14]Department of Clinical Genetics, Erasmus Medical Center, Rotterdam, the Netherlands; [15]Department of Clinical Genetics, Maastricht University Medical Center, Maastricht, the Netherlands; [16]Division of Human Genetics, Children's Hospital of Philadelphia, Philadelphia, PA, USA; [17]Roberts Individualized Medical Genetics Center, Children's Hospital of Philadelphia, Philadelphia, PA, USA; [18]Departments of Pediatrics, Perelman School of Medicine, University of Pennsylvania, Philadelphia, PA, USA; [19]Department of Pathology and Laboratory Medicine, Children's Hospital of the University of Pennsylvania, Philadelphia, PA, USA; [20]Division of Pediatric Neurology, Department of Pediatrics, Gaziantep Islam, Science and Technology University Faculty of Medicine, Gaziantep, Türkiye; [21]Department of Molecular and Human Genetics, Baylor College of Medicine, Houston, TX 77030, USA; [22]Section of Pediatric Neurology and Developmental Neuroscience, Department of Pediatrics, Baylor College of Medicine, Houston, TX, USA; [23]Texas Children's Hospital, Houston, TX 77030, USA; [24]Human Genome Sequencing Center, Baylor College of Medicine, Houston, TX 77030, USA; [25]Department of Pediatrics, Baylor College of Medicine, Houston, TX 77030, USA; [26]Neuroscience and Mental Health Institute, University of Alberta, Edmonton, AB T6G 2E1, Canada; [27]Department of Medical Genetics, University of Alberta, Edmonton, AB T6G 2H7, Canada
[28]These authors contributed equally
*Correspondence: elke.krueger@uni-greifswald.de (E.K.), frederic.ebstein@univ-nantes.fr (F.E.)
https://doi.org/10.1016/j.ajhg.2024.05.016.

The standard functional form of proteasomes is the 26S proteasome, a multi-subunit complex consisting of at least 2 distinct multi-subunit assemblies, namely a 19S regulatory particle (RP) and a 20S core particle (CP).[6,7] While the 19S RP is responsible for recognition, deubiquitinating, and unfolding protein substrates, the 20S CP enables their cleavage into small peptides thanks to its catalytic chymotrypsin-, trypsin-, and caspase-like activities.[8,9] About 50 genes contribute to distinct proteasome isoforms assembly, structure, and function, the large majority of them encoding subunits of the 19S RP (*PSMC1* to *6* and *PSMD1* to *14*) and 20S CP (*PSMA1* to *7* and *PSMB1* to *10*).[10] The ubiquitous and indispensable nature of 26S complexes renders the cell particularly vulnerable to any form of proteasome dysfunction. During aging, a decline in proteasome activity is commonly observed, which, when it falls below a pathological threshold, contributes to late-onset neurodegeneration.[11] Proteasome defects typically disrupt protein homeostasis, leading to the uncontrolled accumulation of ubiquitin-positive protein aggregates, as seen in the brains of individuals with neurodegenerative diseases.[12] Recent evidence has revealed that proteasome dysfunction is not solely limited to aging and neurodegenerative conditions. It can also be observed in young individuals harboring genomic alterations in proteasome genes. Importantly, rare proteasomopathies are associated with 2 distinct clinical phenotypes: proteasome-associated autoinflammatory syndromes (PRAASs) including PRAAS1 (MIM: 256040), PRAAS2 (MIM: 618048), PRAAS3 (MIM: 617591), PRAAS4 (MIM: 619183), and PRAAS5 (MIM: 619175) or neurodevelopmental delay with cognitive impairment and rare inflammatory symptoms, notably encompassing Stankiewicz-Isidor syndrome (STISS) (MIM: 617516).[13] So far, groundbreaking research in this field has shown that recessive variants of *POMP* (MIM: 613386), *PSMG2* (MIM: 609702), *PSMA3* (MIM: 176843), *PSMA5* (MIM: 176844), *PSMB4* (MIM: 602177), *PSMB8* (MIM: 177046), *PSMB9* (MIM: 177045), *PSMB10* (MIM: 176847), and/or *PSMC5* (MIM: 601681), mainly encoding subunits of the 20S CP or assembly helper proteins thereof, were associated with typical signs of autoinflammation such as skin lesions, lipodystrophy, basal ganglia calcifications, and recurrent episodes of fever.[14–23] By contrast, individuals with *de novo* alterations in *PSMB1* (MIM: 602017), *PSMD12* (MIM: 604450), *PSMC1* (MIM: 602706), and *PSMC3* (MIM: 186852), mainly encoding for protein subunits of the 19S RP, were mostly characterized by NDD symptoms ranging from syndromic intellectual disability, skeletal malformations, and failure to thrive to hearing loss or absence of speech without any observable signs of inflammation.[24–30] An emerging view on this conundrum suggests, however, that both PRAASs and NDD share similarities in their molecular pathogenesis with the induction of proteotoxic stress markers and dysregulated type I interferon (IFN) signaling.[31–33]

Here, we strengthen the causal relationship between 19S defects and the development of neurological phenotypes by pinpointing *PSMD11* (MIM: 604449) as a candidate in 10 unrelated subjects exhibiting characteristic manifestations of neurodevelopmental delay. Our findings show that *PSMD11* loss of function correlates with decreased cognitive flexibility in *Drosophila melanogaster*, reduced amounts of 26S proteasome complexes, and the induction of a type I IFN gene signature in T cells from affected individuals, which can be alleviated by small-molecule inhibitors targeting the integrated stress response (ISR).

Material and methods

Genetic studies and ethics statement

This study was approved by the CHU de Nantes ethics committee (research program "Génétique Médicale DC-2011-1399). Written informed consent was obtained for all study participants, probands, and healthy parents. All affected individuals were initially referred for isolated or syndromic developmental delay and/or intellectual disability. They had been evaluated by at least 1 expert clinical geneticist or neurologist in each recruiting center. Variants in *PSMD11* were identified in a research or diagnostic setting after routine genetic testing using the methods described in Table S3. Candidate variants were prioritized and reviewed following the molecular classification guidelines of the American College of Medical Genetics (ACMG) and Genomics and the Association for Molecular Pathology.[34] Upon identification of the first 2 *PSMD11* variants, several subjects were recruited through the online-based platform Genematcher.[35] Variant annotation was made using the free software MobiDetails.[36] The deletion found in subject 10 was identified from single whole-exome sequencing (WES) data using a copy-number variation (CNV) detection algorithm and validated using qPCR probes targeting exons 2 and 14 of *PSMD11*. Read depth for each captured genomic region was calculated with bedtools (version 2.26.0) with a MapQ quality threshold of 20. CNVs were then called using CANOES algorithm on R (v.3.5.2) with default parameters.[37]

Behavioral studies

Drosophila melanogaster flies were reared on a conventional cornmeal-yeast medium developed at Cold Spring Harbor Laboratory.

For the behavioral experiments, we selected *Drosophila* adult flies from different lines, namely w1118 2202U (2U), Elav-Gal4, and a UAS-RNAi line that targeted *PMSD11* ortholog *Rpn6*. The UAS-*Rpn6* RNAi (TRiP) line 29385 was acquired from the Bloomington *Drosophila* Stock Center. To achieve pan-neuronal expression of the RNAi targeting the *Drosophila* ortholog *Rpn6*, we employed the Gal4-UAS system, a widely used spatial restricted expression system. The pan-neuronal driver Elav was utilized to drive the expression of the RNAi construct. Female *Drosophila* adult flies, either Elav-Gal4 or wild-type 2U, were crossed with male UAS-*Rpn6 Drosophila* adult flies.

Following established methods,[38] the *Drosophila* were trained using classical olfactory conditioning to associate an odor with a foot-shock. Our experiment involved placing 100 *Drosophila* adult flies into a training chamber where they were exposed to an odor (odor 1) accompanied by a simultaneous foot-shock for a duration of 60 s. Following a short break, the *Drosophila* were then exposed to a second odor (odor 2) without any shock before being presented with a choice in a t-maze between the 2 odors for a period of 2 min. The number of *Drosophila* adult flies on each side of the

t-maze was recorded. This process was repeated with a new set of 100 *Drosophila* of the same genotype, associating the second odor with the shock. To evaluate performance, we calculated a performance index by dividing the number of *Drosophila* that avoided the shocked odor by the total number of *Drosophila*. For the reversal learning phase, we adopted a similar methodology as described previously.[39] Reversal learning followed a comparable setup and protocol, with the addition of reintroducing the second odor after a 45-s interval, now paired with the shock. This was followed by presenting the first odor without the shock 45 s later and finally the t-maze choice between the 2 odors. Statistical analysis was conducted using ANOVA, followed by Tukey tests using the JMP computer program (purchased from SAS Institute Inc.).

Molecular modeling

To map the different amino acid substitutions of PSMD11 (previously called Rpn6) within proteasome complexes, we utilized the structure of the 19S RP (PDB: 5LN3) as a reference. This mapping process was performed using the freely accessible Swiss PDB-Viewer software.

Cell culture

The peripheral blood mononuclear cells (PBMCs) utilized in this study were obtained from blood samples collected from healthy controls as well as affected individuals along with their parents, if applicable. The isolation of PBMCs involved performing gradient centrifugation using PBMC spin medium (pluriSelect). The isolated PBMCs were then washed 3 times with PBS, frozen in fetal bovine serum (FBS) containing 10% DMSO, and stored in liquid nitrogen for future experimentation. In certain experiments, the collected PBMCs were expanded in U-bottom 96-well plates along with irradiated feeder cells. This T cell expansion was carried out using RPMI 1640 supplemented with 10% human AB serum (both obtained from PAN-Biotech GmbH), interleukin-2 (IL-2) at a concentration of 150 U/ml (Miltenyi Biotec), and L-PHA at a concentration of 1 μg/μL (Sigma) following the procedure of Fonteneau et al.[40] After a culture period of 3–4 weeks, the resting T cells were washed and frozen as dry pellets for further investigations. HEK293T cells, a laboratory stock, were cultured in DMEM supplemented with 10% human AB serum and 1% penicillin/streptomycin. In some experiments, T cells were treated with 1 mg/mL puromycin (Thermo Fisher Scientific) for 3 h.

SDS-PAGE and western blot analysis

Cell pellets from resting T cells isolated from affected individuals, related controls, and healthy individuals were lysed in equal amounts of standard radioimmunoprecipitation assay (RIPA) buffer (50 mM Tris pH 7.5, 150 mM NaCl, 2 mM EDTA, 1 mM N-ethylmaleimide, 10 μM MG-132, 1% NP40, 0.1% SDS), and protein lysates were separated by 10% or 12.5% SDS-PAGE prior to transfer to polyvinylidene fluoride (PVDF) membranes (200 V for 1h). After blocking (20-min exposure to 1× Roti-Block at room temperature), membranes were probed with anti-PSMD11 (clone AT1F4, Santa Cruz Biotechnology), anti-PSMD12 (clone H3, Santa Cruz Biotechnology), anti-PSMC5 (clone p45-110, Enzo Life Sciences), anti-PSMA2 (clone MCP21, Enzo Life Sciences), anti-PSME1 (K232/1, laboratory stock), anti-ubiquitin (clone D9D5, Cell Signaling Technology), and anti-GAPDH (clone 14C10, Cell Signaling Technology) primary antibodies overnight at 4°C under shaking. Subsequently, membranes underwent 3 rounds of washing with PBS/0.2% Tween and were incubated with secondary antibodies (1/5,000 dilution) conjugated to horseradish peroxidase (HRP) targeting either mouse or rabbit antigens for 1 h at room temperature. Proteins were then visualized using a detection kit based on enhanced chemiluminescence (ECL; Bio-rad). Immunoreactive signals were quantified using ImageJ.

Native-PAGE and western blotting

Cell pellets obtained from both affected individuals and controls, consisting of resting T cells, were lysed by employing a native TSDG buffer. The lysis buffer composition included 10 mM Tris pH 7.0, 10 mM NaCl, 25 mM KCl, 1.1 mM $MgCl_2$, 0.1 mM EDTA, 2 mM DTT, 2 mM ATP, and 20% glycerol. Protein extraction was conducted using a non-denaturing approach, which involved subjecting the samples to 5 cycles of freeze/thawing in liquid nitrogen. Soluble whole-cell extracts were obtained, and their protein content was quantified using a standard Bradford assay. Twenty micrograms of protein lysates were loaded onto 3%–12% gradient Bis-Tris gels (Thermo Fisher Scientific) and electrophoresed at 45 V overnight at 4°C in a mixture of 50 mM BisTris and 50 mM Tricine (pH 6.8). For proteasome detection, an in-gel overlay assay was conducted by exposing the gels to 0.1 mM of the suc-LLVY-AMC fluorogenic peptide (Bachem) at 37°C for 20 min in an overlay buffer (20 mM Tris, 5 mM $MgCl_2$, pH 7.0). The bands corresponding to the proteasome were visualized under UV light with a wavelength of 360 nm and captured using an Imager at 460 nm. Subsequently, the native protein complexes were transferred to PVDF membranes (200 V for 1 h), which were then blocked and probed with primary antibodies that specifically target α6 (clone MC20, Enzo Life Sciences) and PSME1 (K232/1, laboratory stock). Immunoreactive signals were quantified using the ImageJ software.

RNA interference

Non-targeting control small interfering RNA (siRNA) (D-001810-10-05) as well as siRNA specific for *PSMD11* (L-011367-01-0005) were purchased from Horizon Discovery Biosciences Limited. The siRNA duplexes were dissolved in 1× siRNA buffer provided by the manufacturer to a final concentration of 20 μM, incubated at room temperature with gentle shaking for 30 min, and then stored at −20°C. Briefly, siRNAs were transiently introduced into HEK293T cells at a final concentration of 50 nM using the JetPRIME transfection reagent (Polyplus) following the supplier's instructions. After 5 days of culture, cells were collected, frozen as dry cell pellets, and stored at −80°C until further use.

Gene expression analysis by NanoString

Total RNA, amounting to 100 ng, was extracted from T cells obtained from both control and affected samples. The extracted RNA was subjected to hybridization using the NanoString nCounter Human AutoImmune Profiling Panel. Subsequently, gene expression quantification was carried out according to the manufacturer's instructions. The obtained data were then normalized to housekeeping genes as per the manufacturer's guidelines.

RNA isolation, reverse transcription, and PCR analysis

Resting T cells were subjected to total RNA isolation with the kit provided by Analytic Jena AG following the manufacturer's instructions. For subsequent real-time PCR analysis, 100–500 ng of the isolated total RNA was reverse-transcribed using moloney murine leukemia virus (M-MLV) reverse transcriptase from Promega. qPCR was conducted using Premix Ex Taq (probe qPCR purchased

from TaKaRa) in duplicate to determine the mRNA expression levels of each IFN-stimulated gene (ISG). FAM-tagged TaqMan Gene Expression Assays obtained from Thermo Fisher Scientific were used for ISG quantification, including *IFI27*, *IFI44*, *IFI44L*, *IFIT1*, *ISG15*, *RSAD2*, *IFI44*, and *MX1*. The real-time PCR reactions were performed following the manufacturer's instructions. The cycle threshold (Ct) values for the target genes were transformed into relative expression values using the relative quantification (RQ) method ($2-\Delta\Delta Ct$). The expression of the target genes was normalized to the Ct values of *GAPDH*. In some experiments, qPCR reactions were performed using self-designed SYBR Green primers to amplify *PSMD11*. Standard thermal cycling and melting curve conditions were employed in a QuantStudio qPCR system (Thermo Fisher) with parallel amplification of GAPDH used to calculate RQ.

Statistical analyses

All charts and statistical analyses were generated using GraphPad Prism v.8. A p value < 0.05 was considered significant.

Sanger sequencing

Primers were designed to PCR amplify the regions covering the c.268C>T (p.Arg90*) and c.612dup (p.Lys205*) variants on *PSMD11* (RefSeq transcript; GenBank: NM_002815.4) generated from total RNA extracted from T cells of subjects 1 and 4. Bidirectional sequencing of the purified PCR products was outsourced to Eurofins Genomics (Nantes, France).

Results

PSMD11 variants cause a neurobehavioral phenotype combining mild developmental delay/intellectual disability and obesity

Ten unrelated subjects presenting with an NDD underwent routine genetic testing, as described in materials and methods. As illustrated in Figure 1A, sequencing analyses across the 10 families revealed the presence of 10 distinct genomic alterations in *PSMD11* (GenBank: NM_002815.4), giving rise to previously undescribed protein changes in the non-ATPase PSMD11 (previously called Rpn6) subunit of the 26S proteasome. Subjects harboring *PSMD11* variants displayed variable degrees of developmental delay, with motor and speech delays almost consistently observed (9/10 individuals). Language developmental disorder was indeed highly observed regardless of the degree of other developmental delays and cognitive phenotype (Table 1). In cases where cognitive and adaptive skill assessments were conducted and available, a majority of affected individuals (4/5) exhibited mild to moderate intellectual disability; notably, subject 9 was described as having a "borderline intellectual disability." It is noteworthy that the father of subject 1, transmitting the c.268C>T (p.Arg90*) variant, and the mother of subject 7, harboring the c.788+2T>C splice variant, were reported by clinicians and/or relatives to have experienced developmental delays, mild cognitive impairment, learning disabilities, or psychiatric disorders. The father of subject 2, carrying the c.268C>T (p.Arg90*) variant, was reported by relatives as having a mild intellectual disability with learning difficulties and slow speech (Table S1).

Subject 6 exhibited the most severe presentation, possibly influenced in part by premature birth and associated comorbidities. Notably, West syndrome was also diagnosed, which exacerbated during multiple infectious episodes. Brain imaging was conducted for only 3 subjects, revealing various anomalies in 2 cases. In particular, subject 6 exhibited germinal matrix and intraventricular hemorrhage, which have been associated to his premature birth, and a pontocerebellar hypoplasia, not found in other explored individuals. Cerebral imaging was not indicated in the remaining subjects.

As depicted in Table 1, abnormal behavior emerged as a predominant neuropsychiatric symptom within our series, affecting 8 out of 10 subjects. Specifically, autism spectrum disorder (ASD) was observed in nearly half of the cases, affecting 4 of 10 subjects. Among the cohort of affected individuals, only 1 exhibited short stature (height <2 standard deviations [SDs]), while 5 out of 10 were affected by overweight (1/5) or obesity (4/5).

Interestingly, there was no discernible correlation between short stature and body mass index (BMI). Nevertheless, the overall median SD in height for the series was relatively low at −1.37 SD, indicating a tendency toward shorter stature (Center for Disease Control height-for-age growth chart, https://www.cdc.gov/growthcharts/index.htm). Remarkably, hyperphagia was observed in subject 1 and likely played a significant role in contributing to the observed weight, yet it was not reported that other subjects affected by obesity showed an abnormal consumption behavior. Besides obesity, the 5 subjects exhibited various endocrinological features, including conditions such as diabetes, dysthyroidism, and early puberty (subsequent to obesity for the latter). The presence of early insulin resistance, type 2 diabetes, and/or hypertension in subjects 1 and 8, respectively, aged 15 and 14 years, underscored the severity of obesity (Table 1 and Table S1). Although several distinctive facial features were noted, they did not provide a clear basis for identifying a common facial dysmorphism, as illustrated in Table S2. Importantly, no distinct common organ abnormalities, malformations, or neurosensorial features were identified among the subjects. Manifestations of Bardet-Biedl syndrome (MIM: 615986) in subject 2, as seen in Table S1, were typical and were not included in the description of the *PSMD11*-related NDD. Milder phenotype observed in the father only carrying the p.Arg90* variant seems more consistent with the rest of the individuals described (see supplemental note: case reports).

PSMD11 variants impairing neurodevelopment are mainly loss of function

Remarkably, aside from 2 inherited compound missense variants c.788C>T (p.Thr263Ile) and c.914C>T p.(Ala305Val) identified in subject 6, all other alterations displayed a consistent pattern of dominant loss-of-function variants arising from protein truncation or deletion. Indeed, 7 out

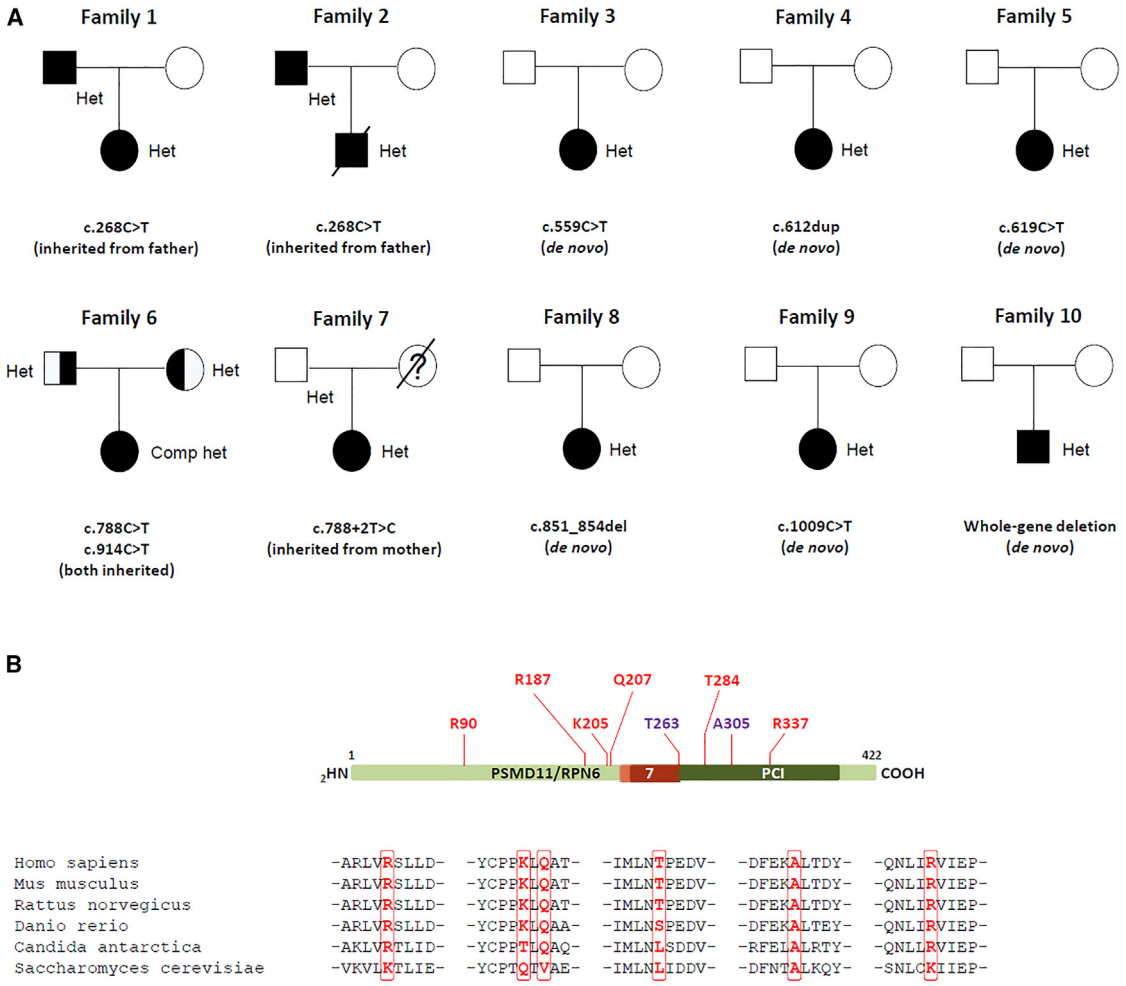

Figure 1. Family pedigrees and cross-species alignment of the regions of the PSMD11 proteasome subunit subjected to missense variants

(A) Pedigrees of the 10 affected families carrying variants in *PSMD11*. Male and females are indicated by squares and circles, respectively. Affected individuals are denoted by filled symbols. Healthy heterozygous carriers are highlighted by a half-filled symbol.

(B) Schematic representation of the PSMD11 protein primary structure showing the distribution and localization of the residues subjected to missense (purple) or loss-of-function (red) variants. Exon 7 is predicted to be abnormally spliced in subject 7, marked in red. The proteasome component (PCI) domain is marked in dark green. The lower panel shows multiple sequence alignment of PSMD11 regions prone to amino acid substitutions across species.

of 10 of the *PSMD11* lesions led to a premature termination codon. These included c.268C>T (p.Arg90*), inherited from mildly affected fathers in both subjects 1 and 2, and *de novo* unique alterations c.559C>T (p.Arg187*), c.612dup (p.Lys205*), c.619C>T (p.Gln207*), c.851_854del (p.Thr 284Lysfs*3), and c.1009C>T (p.Arg337*) in subjects 3, 4, 5, 8, and 9, respectively. Other variants included (1) the intronic alteration c.788+2T>C in subject 7, predicted to result in the skipping of exon 7 and a frameshift in the coding sequence and found in the mother showing a neurobehavioral and psychiatric disorder, as detailed in Table S1; and (2) a deletion encompassing the entire gene in subject 10. In addition, subject 1 also carried a likely pathogenic variant in *PSMC5*, while subject 2 was diagnosed with Bardet-Biedl syndrome, attributable to the identification of a homozygous pathogenic variant in *BBS9* (MIM: 607968), which partly contributes to the phenotype.

As *PSMD11* is predicted to be highly intolerant to loss-of-function variants, with a probability of being loss-of-function intolerant (pLI) = 1 (GnomAD v.4, threshold ≥ 0.90); observed/expected (o/e) ratio = 0.02 ([0.01–0.08] 90% confidence interval [CI], threshold <0.35), the aforementioned variants were selected as prime candidates likely causing the phenotype in the affected individuals. ACMG criteria for each variant are detailed in Table S2. As depicted in Figure 1B, most of these alterations were distributed throughout the PSMD11 primary structure, and the affected amino acids and/or regions showed a high evolutionary conservation across species from human to zebrafish. The *de novo* 17q11.2 deletion identified in subject 10, which excluded *NF1* (MIM: 613113), encompassed 3 non-OMIM morbid genes (Figure S1), with *PSMD11* emerging as a robust candidate (highest pLI, lowest o/e ratio, and predicted haploinsufficiency).

Table 1. Clinical recap of main features in 10 individuals carrying a *PSMD11* variant

Sex	**F = 8**	**M = 2**
Age	**2 years, 2 months–22 years**	
Growth		
Low birth weight (<10 percentile)	2	
Microcephaly (≤−2 SD)	1	
Macrocephaly (≥2 SD)	1	
Short stature (≤−2 SD)	1	
Overweight (>85 percentile/age)	5	
Obesity (>95 percentile/age)	4	
Neurobehavioral		
Intellectual disability (/assessed)	5/8	
Borderline/mild	1	
Moderate	3	
Severe/profound	1	
Developmental delay	10	
Motor delay	9	
Speech delay	9	
Abnormal behavior	8	
Autism/ASD	4	
ADHD	3	
Hyperphagia	1	
Seizures	2	
Developmental regression	2	
Abnormal brain imaging (/assessed)	3/4	
Other miscellaneous findings		
Ophthalmological[a]	3	
Early puberty	F = 2	M = 0
Diabetes/insulin resistance	2	
Dysthyroidya	2	
Constipation	2	

[a]Excluding subject 2 (BBS9-related Bardet-Biedl syndrome).

Two overlapping deletions affecting the same 3 genes (*PSMD11*, *CDK5R1* [MIM: 603460], and *MYO1D* [MIM: 606539]) have been documented. One instance is cataloged in the Control Database of Genomic Variation (DGV; ID: nsv519839), while another is reported in the literature and linked to autism.[41]

Structural mapping predicts disruptive effects of *PSMD11* variants on 26S proteasome complex assembly

To assess the structural implications of the 10 identified *PSMD11* variants on the 26S proteasome, we analyzed the spatial arrangement of the affected protein regions using the structure generated by Schweitzer et al. (PDB: 5LN3).[42] As shown in Figure 2A, the PSMD11 subunit was positioned on the outer surface of the 26S complex, extending notably toward both the 20S and 19S particles and acting as molecular clamp.[43] Our three-dimensional *in silico* mapping revealed that the regions undergoing alterations included interaction sites enabling the precise docking of PSMD11 onto the α-ring of the 20S CP (Figure 2B), as well as onto specific ATPase subunits of the base (Figure 2C) and non-ATPase subunits of the lid (Figure 2D) within the 19S RP.

As depicted in Figure S2, PSMD11 was positioned in close proximity to the PSMA2, PSMD12, PSMD6, PSMC4, and PSMC5 subunits of the 26S complex. A detailed examination of the 26S proteasome structure revealed that the interaction between PSMD11 and its neighboring

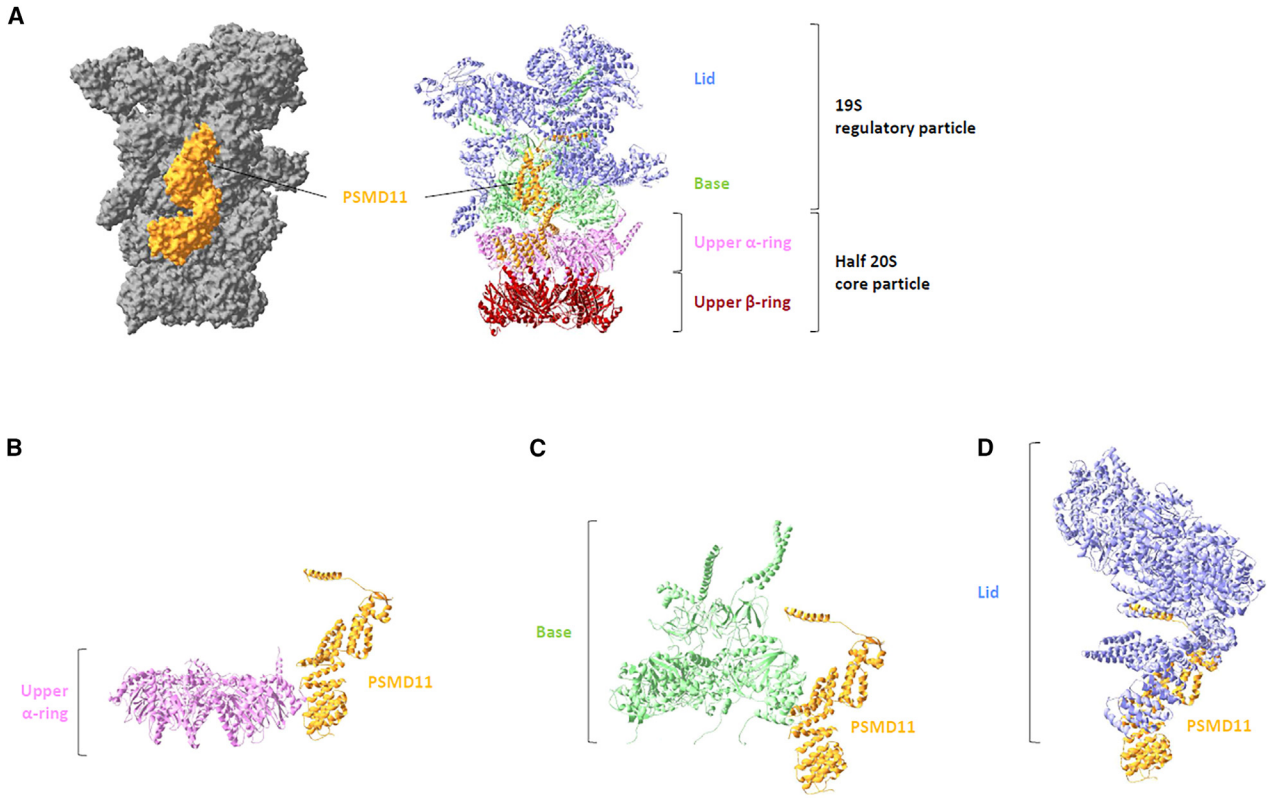

Figure 2. ***In silico*** **protein structure analysis of the PSMD11 subunit affected regions within proteasome complexes**
(A) Cryo-electron microscopy (EM) structure of the human 26S proteasome without imposed symmetry (PDB ID: 5LN3) containing the PSMD11 subunit marked in orange. Right: the lid and the base of the 19S regulatory particle are shown in ribbon colored in light blue and green. The α- and β-rings of the upper half of the 20S core particle are shown in ribbon colored in pink and brown, respectively. (B–D) Bottom: lateral view of the PSMD11 subunit interacting with the upper α-ring (*B*), base (*C*), and lid (*D*) of the 19S regulatory particle, as indicated.

PSMD12 and PSMD6 subunits of the lid was primarily mediated by the very C-terminal segment of the PSMD11 full-length protein (Figure S2). This suggests that all 7 truncating alterations in PSMD11, occurring downstream of this binding region, are predicted to disrupt these interactions, provided that these variants evade nonsense-mediated mRNA decay (NMD) and sustain stable expression at the protein level.

PSMD11 nonsense and frameshift variants do not evade NMD in subject-derived cells

To investigate whether the truncating *PSMD11* variants are subjected to NMD, we subsequently PCR-amplified *PSMD11* from subjects 1 and 4 expressing the c.268C>T (p.Arg90*) nonsense and c.612dup (p.Lys205*) frameshift variants, respectively, followed by Sanger sequencing. As illustrated in Figure S3A, both subjects exhibited reduced levels of *PSMD11* transcripts compared to healthy individuals, as determined by RT-qPCR. Strikingly, sequencing analysis revealed that the expressed *PSMD11* mRNA in both subjects was of wild-type nature (Figure S3B), suggesting that only the intact allele was expressed, while transcripts carrying the c.268C>T and c.612dup alterations, encoded by the damaged alleles, were directly targeted for NMD. To further validate the involvement of NMD in this process, we subsequently treated subject-derived T cells with puromycin, a translation inhibitor recognized for its capacity to suppress NMD.[44] Our data show that puromycin treatment restored the supply of mRNA encoding the c.268C>T (p.Arg90*) and c.612dup (p.Lys205*) *PSMD11* variants in subjects 1 and 4, respectively, as confirmed by Sanger sequencing analysis (Figure S3B). These data demonstrate that the c.268C>T and c.612dup mRNA variants undergo NMD, leading to *PSMD11* haploinsufficiency. Consequently, any potential structural impacts of the truncating variants on the 26S proteasome complex are relevant solely in the context of impaired NMD.

PSMD11 silencing is associated with impaired proteasome function

Considering the haploinsufficiency nature of the *PSMD11* truncating variants, our next objective was to assess the effects of insufficient PSMD11 protein levels on proteasome function. To achieve this, we employed a siRNA-based strategy to silence *PSMD11* in HEK293T cells before proceeding with protein extraction and the analysis of proteasome contents and activities. As depicted in Figure S4, cells subjected to *PSMD11* knockdown exhibited decreased

chymotrypsin-like activity in their 30S, 26S, and 20S proteasome complexes, as assessed by in-gel overlay analysis. This correlated with a decrease in the levels of the 26S proteasome complexes, as indicated by staining the gel against the constitutive PSMD12 proteasome subunit of the lid. As expected, the reduced proteasome pools were associated with an increased accumulation of ubiquitin-modified proteins (Figure S4). Altogether, these data conclusively demonstrate that the PSMD11 subunit is essential for proteasome assembly to maintain protein homeostasis.

Reversal learning memory is impaired in *Drosophila* with a knockdown of *Rpn6*

Given the neurological manifestations associated with *PSMD11* variants, we sought to investigate the potential role of the corresponding subunit in cognitive function. To address this question *in vivo*, we evaluated the learning performance of *Drosophila* in which the expression of *Rpn6* (the *Drosophila* ortholog of human *PSMD11*) was suppressed using RNAi silencing. This approach, which has been proven reliable for efficient and specific *Rpn6* knockdown,[45] was driven by the neuron-specific embryonic lethal abnormal visual system (Elav) promoter. As depicted in Figure 3A, the experimental setup consisted of a widely recognized olfactory classical conditioning in which the animals were trained to learn the contingency between 1 specific odor (4-methylcyclohexanol, MCH) and the aversive effects of an electric shock, as previously described.[29] To confirm that the avoidance response was triggered by the shock itself rather than the odor of a peculiar product, we conducted a repeat experiment with a separate group of *Drosophila* exposed to a different odor, specifically 3-octanol (OCT).

Interestingly, our data show that *Rpn6*-depleted *Drosophila* performed in a comparable manner to their wild-type counterparts during the initial discrimination task (Figure 3B). However, the former displayed a significant decline in their ability to adapt their behavior to inverted odor-shock pairing (Figure 3C), indicating that *Rpn6* loss of function interferes with the process of reversal learning. These findings support the inference that the *PSMD11* ortholog, *Rpn6*, is essential in behavioral flexibility in *Drosophila*.

PSMD11 variants impair proteasome activity and assembly

To further explore the pathogenicity of the *PSMD11* variants, we analyzed T cells from subjects 4, 7, and 6 to assess their proteasome content and activity using in-gel fluorescence assay followed by western blotting on native-PAGE. As illustrated in Figures 4A and 4B, aside from subject 7, whose chymotrypsin-like activity of the 26S and 20S proteasome complexes was reduced compared to controls, no discernible differences were observed in the ability of proteasomes to hydrolyze the LLVY-AMC fluorogenic peptide between affected individuals and controls. Subsequent western blot analysis using antibodies specific to the α6 and PA28-α subunits revealed that the decreased 26S activity observed in subject 7 was attributable to a reduced amount of 26S and/or hybrid proteasomes (Figure 4A). Remarkably, the pool of these complexes was also diminished in all T cell samples carrying *PSMD11* variants, including those derived from subject 6's parents, who were clinically healthy (Table S1). As shown in Figure 4A, the lowest levels of 26S and hybrid proteasomes were evident in T cells from subjects 7 and 6. Intriguingly, these reductions coincided with a slight upregulation of their 20S and 20S-PA28 proteasomes (Figure 4A). With the exception of these 2 subjects, *PSMD11* variants predominantly influenced 26S and/or hybrid proteasome complexes, with minimal to no impact on latent or 20S-PA28 proteasomes. Densitometric analysis revealed that individuals with *PSMD11* variants exhibited an average reduction of approximately 50% in 26S and hybrid proteasome levels compared to healthy donor controls. In summary, these findings strongly suggest that the identified *PSMD11* genomic alterations were loss-of-function variants that primarily affect the intracellular abundance of functional 26S and hybrid proteasomes by perturbed proteasome assembly.

PSMD11 variants differentially impact PSMD11 subunit steady-state expression and phosphorylation pattern

To investigate whether proteasome deficiencies associated with the *PSMD11* variants were attributed to defects in subunit expression, we assessed T cells for their proteasome subunit contents by SDS-PAGE and western blotting. Staining for PSMD11 revealed a double band, indicative of post-translational modifications (Figure 5A). This accumulation pattern aligns with previous studies, wherein increased phosphorylation is suggestive of augmented proteasome assembly and/or activity.[46,47] Notably, the steady-state expression of unmodified and/or phosphorylated (p) PSMD11 was severely affected in T cell samples harboring *PSMD11* variants. While truncating variants of subjects 7 and 4 were associated with reduced levels of unmodified PSMD11, possibly due to a monoallelic PSMD11 accumulation, missense variants in subject 6 and her parents led to decreased phosphorylation of PSMD11 (Figures 5A and 5B). Moreover, the effects on (p)PSMD11 were more pronounced for the biallelic variants in subject 6 than for the monoallelic variants in subject 6's father and mother (Figures 5A and 5B). No endogenous truncated species were detected in the subject samples carrying nonsense mutations, likely due to NMD and/or the fact that the anti-PSMD11 antibody used in this study targets the C-terminal region of the full-length protein.

On the other hand, the steady-state accumulation levels of PSMD12 remained relatively consistent between affected individuals and controls, suggesting that the supply of 19S regulatory subunits of the lid was unaffected by any of the 5 investigated *PSMD11* variants under these conditions. Likewise, none of the *PSMD11* variants exerted a discernible effect on the intracellular content of PA28α,

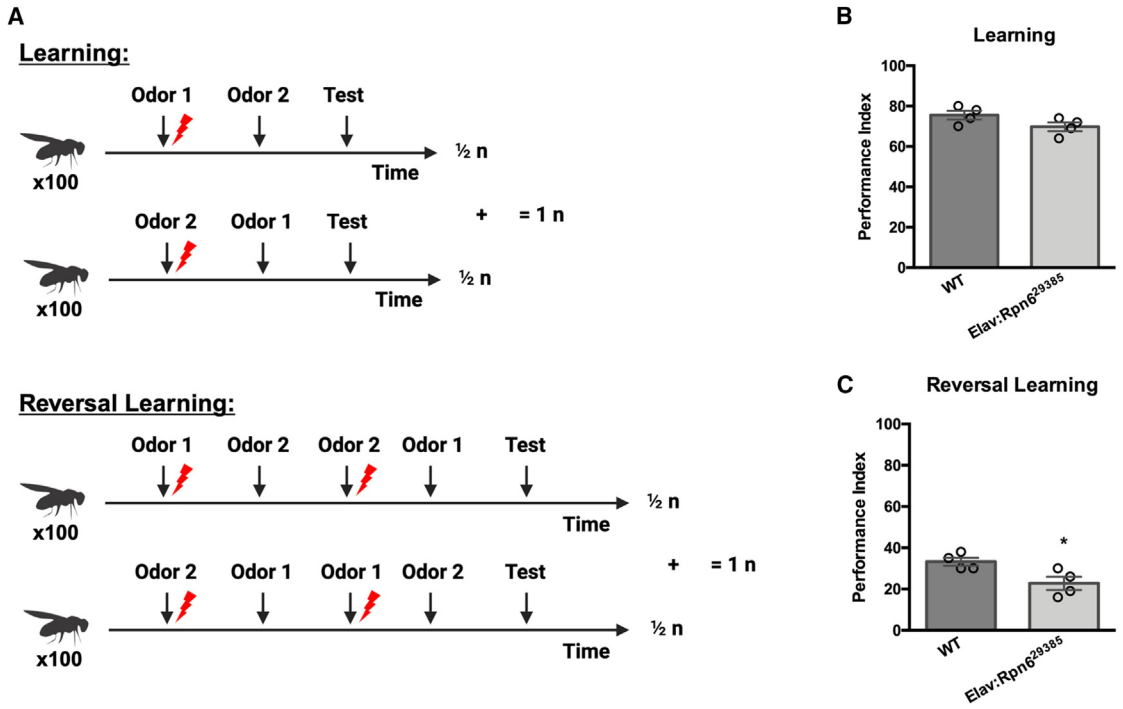

Figure 3. ***Rpn6*** **knockdown (KD) affects reversal learning in** ***Drosophila***

(A) Schematic of olfactory learning and reversal learning. Classical olfactory conditioning consisted of 100 *Drosophila* learning the contingency between odor 1 being paired with electric shock and odor 2 with no shock ($^1/_2$ n). Another 100 naive *Drosophila* were then trained with the reverse odor and shock pairing to counter any odor preference ($^1/_2$ n). Combining these 2 results was considered $n = 1$. Reversal learning consisted of the same initial training cycle but added a second training cycle immediately after that would reverse the odor and shock pairing from the first training.

(B) For learning, the learning performance index (PI) of wild-type and pan-neuronal (Elav) *Rpn6*-KD *Drosophila* did not differ significantly ($N = 4$; t test, $p = 0.1136$).

(C) Conversely, *Rpn6*-KD *Drosophila* performed significantly worse than wild-type *Drosophila* on the reversal learning paradigm ($N = 4$; t test; $p = 0.0314$).

indicating that the reduced levels of hybrid proteasomes in these subjects resulted from an assembly defect rather than a shortage of PA28 subunits. Interestingly, the levels of free PSMC5 and PSMA2 remained intact in subjects 4 and 6, whereas they were severely reduced in subject 7 compared to controls. These data indicate that the decreased levels of 26S proteasomes in subjects 4 and 6 were due to the failure of these cells to assemble such complexes, whereas those of subject 7 were additionally due to a reduced production of the individual subunits of the 20S CP and ATPases of the base of the 19S RP. Collectively, these findings highlight that the mechanisms by which *PSMD11* variants interfere with the pools of 26S and hybrid proteasomes follow distinct paths.

PSMD11 variants induce a type I IFN gene signature in sterile conditions in T cells from affected individuals

We next sought to determine whether the identified *PSMD11* alterations aligned with previously described proteasome loss-of-function variants in their ability to generate specific type I IFN gene signatures, as shown for proteasomopathies.[13] To address this point, we utilized the Nanostring nCounter Human AutoImmune Profiling Panel to assess the immune transcriptome of T cells derived from subjects 7 and 4 to that of 3 unrelated healthy individuals. As depicted in Figure 6A, we identified 30 differentially expressed genes between control and subject samples, including a group of 10 ISGs (*IFI27* [MIM: 600009], *IFI35* [MIM: 600735], *IFI44* [MIM: 610468], *IFI44L* [MIM: 613975], *IFIT1* [MIM: 147690], *ISG15* [MIM: 147571], *MX1* [MIM: 147150], *OAS1* [MIM: 164350], *OAS2* [MIM: 603350], and *RSAD2* [MIM: 607810]) consistently upregulated in individuals with *PSMD11* variants. Other genes with constitutively induced transcription rates in subject T cells included components of the IL-27 signaling pathway, such as *IL27RA* (MIM: 605350) and *IL6ST* (MIM: 600694), as well as *AHR* (MIM: 600253), encoding ligand-activated transcription factor AhR of the xenobiotic response (Figure 6A). Remarkably, *PSMD11* loss of function was also associated with a strong downregulation of histone gene expression, particularly concerning genes of the core histones H2A, H2B, H3, and H4 (Figure 6A), suggesting potential genomic instability.

To confirm the association of *PSMD11* variants with the emergence of type I IFN responses, we further analyzed the transcription rate of 7 ISGs in subjects 1, 4, 6, and 7 by quantitative PCR, as previously described.[26,29] All 4 investigated subjects exhibited at least a 4-fold increase in their

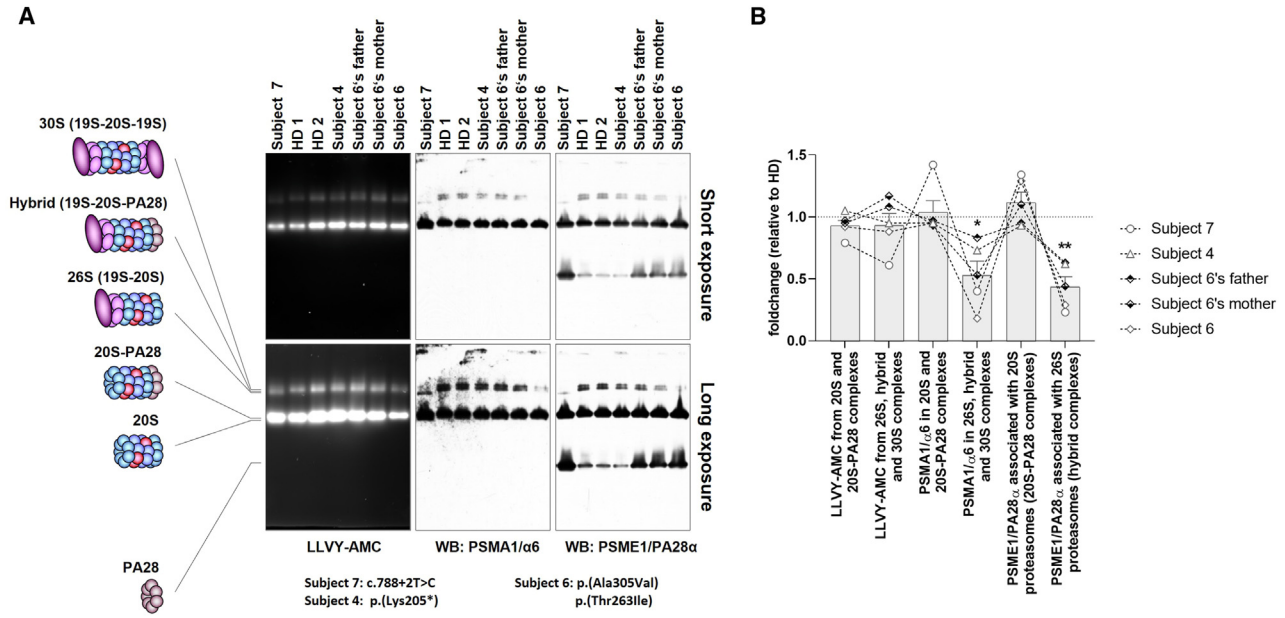

Figure 4. T cells carrying *PSMD11* variants exhibit reduced amounts of 26S, hybrid, and 30S proteasome complexes

(A) Twenty micrograms of T cell lysates from subjects 2, 4, and 6 as well as both parents of subject 6 and 2 unrelated healthy donors (HDs) were separated by 3%–12% native-PAGE. Proteasome chymotrypsin-like activity was assessed in gels using the LLVY-AMC fluorogenic reporter substrate, as indicated. Gels were subsequently subjected to western blotting using antibodies specific for PSMA1 and PSME1, as indicated. The left schematic illustrates the proteasome complexes (30S, hybrid, 26S, 20S-PA28, and 20S) and free regulators (19S and PA28) detected using the 2 antibodies.

(B) Quantification of the LLVY-AMC fluorescent signals and PSMA1 and PSME1 immunoreactive bands in 20S, 20S-PA28, 26S, hybrid, and/or 30S proteasome complexes by densitometry, as indicated. Data are presented as activity (LLVY-AMC) and protein (PSMA1 and PSME1) fold changes in subjects 2,4, and 6 as well as both parents of subject 6 vs. healthy donors (HDs) whose densitometric measurements were set to 1 (gridline), as indicated. Columns indicate the fold change mean values ± SEM calculated from the 5 normalizations. Statistical significance was assessed by unpaired Student's test (*$p < 0.05$, **$p < 0.01$).

ISG mRNA levels compared to healthy individual controls (Figure 6B). Specifically, the most strongly upregulated genes across all subjects included *IFIT1*, *IFI27*, *IFI44*, and *IFI44L*, whereas *ISG15*, *MX1*, and *RSAD2* showed only modest induction. Interestingly, subjects 7 and 4 displayed the most potent type I IFN signatures, showing a 25- and 40-fold ISG upregulation, respectively, followed by subjects 1 and 6, whose ISG increase did not exceed 5-fold compared to healthy donors (Figure 6B). Remarkably, our data also revealed that subject 6's parents, who carried monoallelic missense variants in *PSMD11* and were clinically healthy, developed an IFN signature comparable to that of their offspring (Figure 6B). This suggests a potential role of these variants in inducing type I IFN responses, even in individuals without apparent clinical symptoms.

The type I IFN signature generated in T cells with *PSMD11* variants is triggered by the ISR

To refine our assessment of the propensity of T cells with *PSMD11* variants to generate a type I IFN gene signature, we calculated and compared the IFN scores of affected individuals and their related controls to those of T cells isolated from 6 healthy donors. The calculation of IFN scores followed the established procedure outlined in Rice et al.'s study.[48] As shown in Figure 7A, all 4 investigated subjects were endowed with higher IFN scores than those of the 6 unrelated healthy individuals, which were far below the cut-off value of 2.466. Consistent with our previous observations, we noted that both parents of subject 6 (Figure 7A), despite being clinically asymptomatic, displayed positive IFN scores. This finding further reinforces the potential role of *PSMD11* variants in driving the activation of type I IFN responses, regardless of whether individuals develop overt clinical symptoms.

In an effort to pinpoint the mechanisms by which the loss of *PSMD11* function triggered sterile type I IFN responses, we next tested a series of small-molecule inhibitors on T cells derived from subjects 1, 6, and 7. Based on previous studies that pointed to the roles of the unfolded protein response (UPR) and ISR in conferring type I IFN gene signatures in response to proteasome dysfunction,[29,31,49] we tested the impact of specific inhibitors of these pathways. The inhibitors used in our study included 4μ8C and C16, selectively targeting IRE1α (*ERN1* [MIM: 604033]) within the unfolded protein response (UPR), and protein kinase R (PKR) (*EIF2AK2* [MIM: 176871]) within the ISR, respectively. In addition, considering that proteasome dysfunction has been shown to influence the turnover of mitochondria,[50] potentially leading to the release of mitochondrial DNA into the cytosol, we further explored the effects of H-151, an inhibitor of the cytosolic DNA sensor STING (*STING1* [MIM: 612374]). Remarkably,

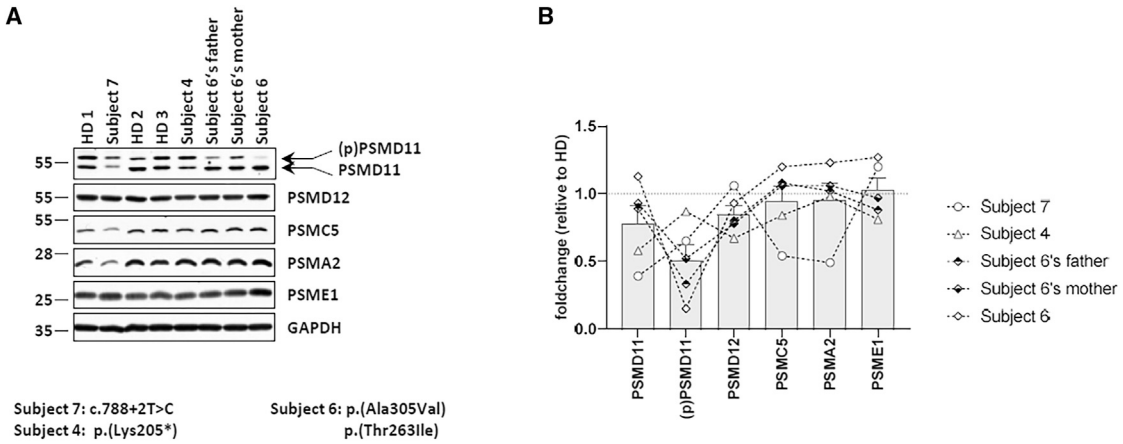

Figure 5. *PSMD11* variants affect the steady-state expression level of unmodified and/or phosphorylated PSMD11 proteins
(A) Five to 20 micrograms of RIPA lysates from T cells isolated from subjects 2, 4, and 6 as well as both parents of subject 6 and 3 unrelated healthy donors (HDs) were separated by SDS-PAGE followed by western blotting using antibodies specific for PSMD11, PSMD12, PSMC5, PSMA2, PSME1, and GAPDH (loading control), as indicated.
(B) Quantification of the western blots by densitometry. Data are presented as fold changes in subjects 4, 6, and 7 as well as both parents of subject 6 vs. healthy donors (HDs) whose densitometric measurements were set to 1 (gridline), as indicated. Columns indicate the fold change mean values ± SEM calculated from the 5 normalizations.

while the ISG expression profile of *PSMD11* subjects did not substantially vary following treatment with IRE1α inhibition by 4μ8C, it was severely reduced by the PKR inhibitor C16, clearly indicating the involvement of PKR in the induction of type I IFN-driven gene signatures (Figure 7B). Inhibition of STING by H-151 resulted in a decrease of the IFN score, but this was less pronounced compared to PKR inhibition, suggesting that cytosolic DNA makes only a minor contribution to IFN production under these conditions. These data implicate the ISR in the development of type I IFN response upon proteasome dysfunction caused by *PSMD11* loss-of-function variants.

Discussion

In this study, we identified *PSMD11* as an additional member of the growing family of proteasome genes associated with neurodevelopmental phenotypes, alongside *PSMB1*, *PSMC1*, *PSMC3*, and *PSMD12*. The phenotype of individuals with *PSMD11* variants differed from those reported previously in other autosomal-dominant proteasome-associated NDDs, including those caused by variants in *PSMD12* or *PSMC3*.[24,25,29] This expands the phenotypic spectrum of the neurodevelopmental proteasomopathies initially described by Cuinat et al.[33]

In this series, the disorder associated with *PSMD11* variants generally did not involve multiple systems, except for subject 2, who presented with manifestations related to Bardet-Biedl syndrome (Table S1). Of note, subject 1 and 2 both carried a second molecular event explaining part of their phenotype. With the implementation of whole-genome sequencing and WES as a first-line tool in the diagnosis of NDDs, the establishment of a dual molecular diagnosis has become more common. This "dual diagnosis," or multilocus pathogenic variation (MPV), often accounts for entangled or atypical presentations,[51–53] as seen in subject 2, who displayed obvious Bardet-Biedl syndrome manifestations. The presence of the *PSMD11* variant in the respective fathers of subjects 1 and 2, without second event and presenting with a mild non-syndromic intellectual disability, was consistent with the findings in other described subjects. Furthermore, the molecular *in vitro* impact of the c.268C>T (p.Arg90*) variant, as inferred from the tests on T cells from subject 1's father, aligned with the results obtained for the other tested *PSMD11* variants.

We did not detect concurrent cardiac, renal, genital, or skeletal congenital abnormalities in any *PSMD11* subjects, nor did we observe hearing loss, which were frequently observed in individuals with *PSMD12* or *PSMC3* variants.[26,29] Similarly, ophthalmological findings were both less prevalent and less severe, primarily manifesting as strabismus, in cases with *PSMD11* variants (4/10) as opposed to those with *PSMD12* variants.[24,26] While there was evident phenotypic variability among individuals, certain consistent features of this disorder emerged. Notably, all subjects exhibited impaired neurodevelopment, characterized by speech delay, motor delay, and behavioral issues (Table 1). However, the cognitive phenotype observed in this study appeared to be milder in comparison to previously described neurodevelopmental proteasomopathies. Hence, the proportion of variants inherited from a mildly affected parent was higher than what has been observed in *PSMC3*-related disorders and *PSMD12*-related disorders (STISS).[24,26,29]

Another noteworthy characteristic of this disorder was overweight body habitus in 50% of cases, with an occurrence of a severe early-onset obesity affecting 4 out of 10 cases (Table 1). Intriguingly, changes in lipid metabolism

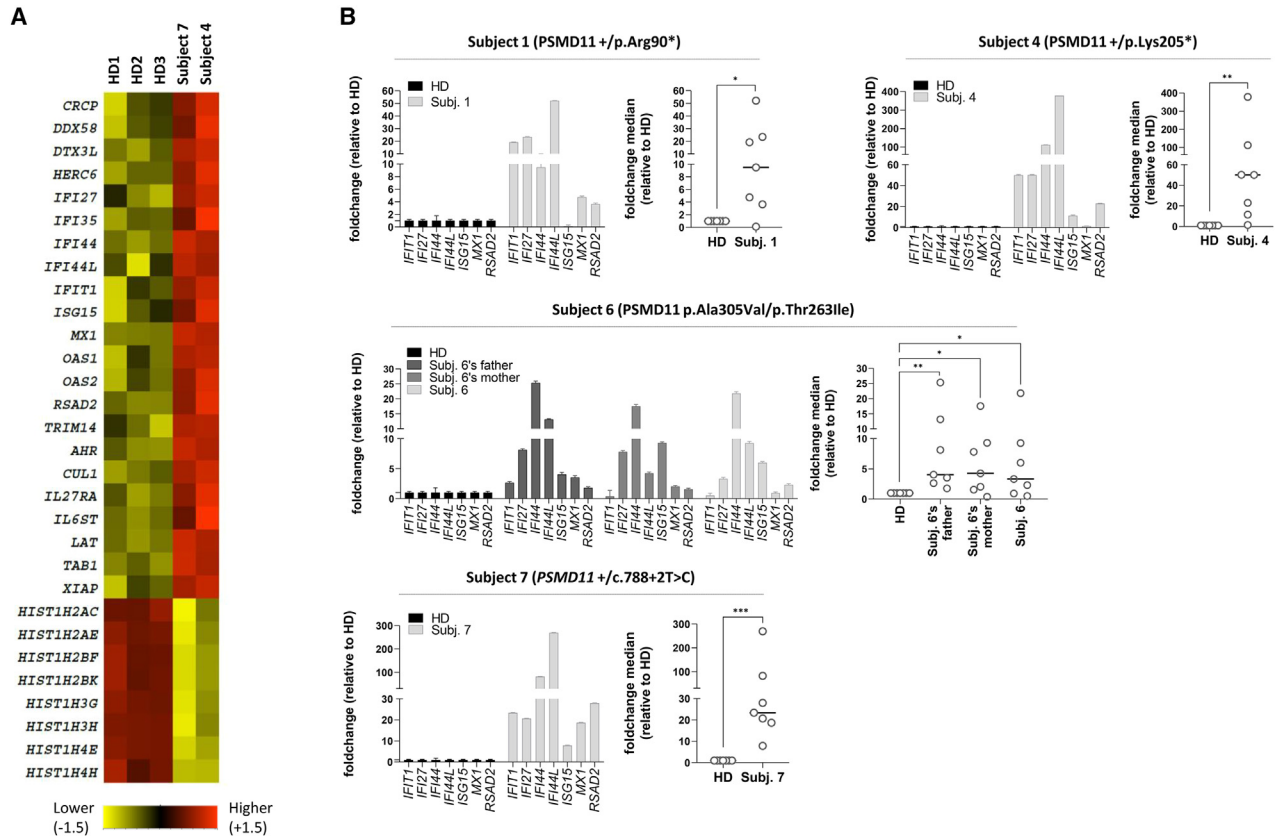

Figure 6. T cells from subjects with *PSMD11* variants develop a type I interferon (IFN) gene signature

(A) Non-clustered heatmap visualization of gene expression in T cells isolated from subjects 4 and 7 carrying *PSMD11* variants and 3 unrelated healthy donors (HDs). Each column represents 1 individual subject or control and each row represents 1 gene. Color indicates normalized counts of each transcript, with red representing higher expression and yellow relatively lower expression.

(B) Gene expression of 7 IFN-stimulated genes (ISG, namely *IFIT1*, *IFI27*, *IFI44*, *IFI44L*, *ISG15*, *MX1*, and *RSAD2*) was assayed by RT-qPCR on T cells derived from subjects 1, 4, 6, and 7 as well as both parents from subject 6 and healthy donor (HD) controls. Expression levels were normalized to *GAPDH* and relative quantifications (RQs) are presented as fold change over controls. Shown is also the median fold expression of the 7 ISG over healthy donors (HDs). Statistical significance was assessed by ratio paired t test where * indicates $p < 0.05$, ** indicates $p < 0.01$ and *** indicates $p < 0.001$.

have not been documented in previously reported cases of neurodevelopmental proteasomopathies. Nonetheless, given the limited sample size of subjects, the assessment of weight-related health issues requires additional confirmation. This is particularly relevant considering that lipid metabolism is clearly affected in PRAAS, leading to the onset of conditions like lipodystrophy and metabolic syndrome in certain cases.[15,20,54]

Our study unequivocally shows that *PSMD11* loss-of-function variants in these cells lead to proteasome malfunctions, culminating in a discernible type I IFN gene signature (Figure 6). This not only reinforces earlier observations associating NDD caused by 19S RP variants with type I interferonopathies[26,29] but also establishes a potential connection with metabolic regulation, as type I IFN serves as a prominent regulator of processes related to obesity, including the regulation of adipocyte and hepatocyte inflammation, stress response, and modulation of food intake.[55–58] IFN response also has a major role in the appearance of the remodeling of adipose and hepatic tissue involved in insulin sensitivity and resistance, which contributes to the elevated risk of type 2 diabetes in obesity.[55,57,59,60] Additionally, our findings indicate a close interrelation between the activation of a type I IFN response and the ISR, underscored by the marked reduction in IFN response observed when employing inhibitors of PKR (Figure 7B). It is worth noting that prior studies have already established a correlation between the ISR and obesity,[55,58] providing specific evidence implicating PKR in the onset of this condition.[56,61,62] Regarding PKR, our findings align with a comparable involvement in the type I IFN response, as observed in individuals with NDD carrying a *PSMC3* variant[29] and individuals with PRAASs.[14,15,20,63] Although the mechanism of PKR activation by proteasomal loss of function has not been thoroughly explored, it likely involves the uncontrolled accumulation of ubiquitin-modified proteins, including IL-24, as previously suggested.[49]

Another consistent feature of T cells with *PSMD11* alterations is their reduced content of 26S and hybrid proteasomes (Figure 4A), a finding that was also observed and confirmed using *PSMD11*-depleted HEK293T cells

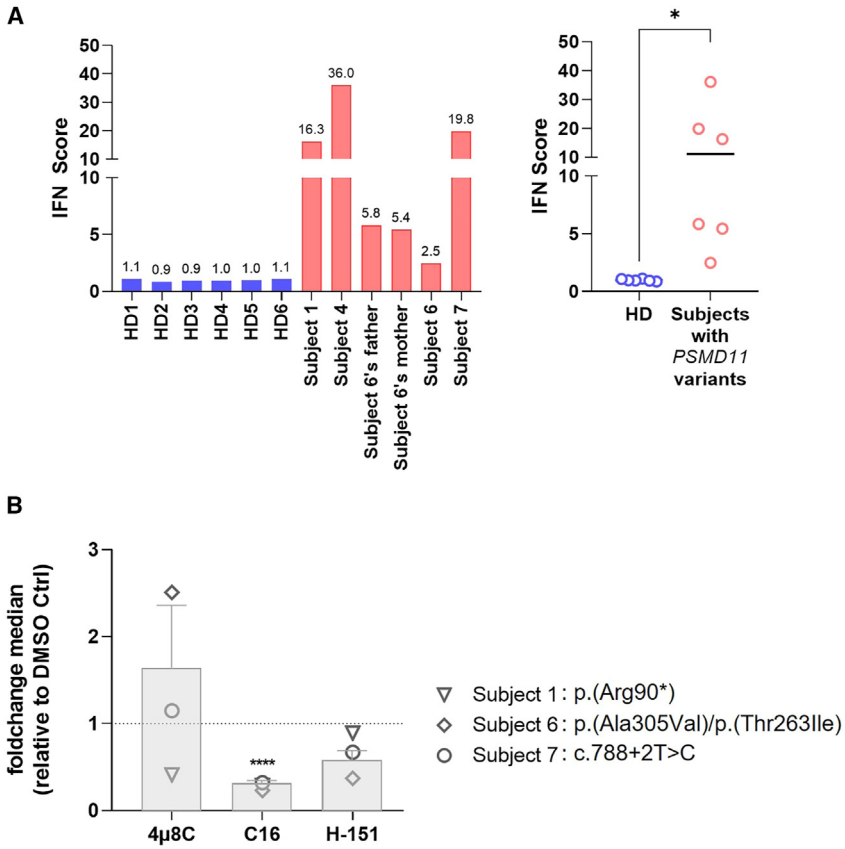

Figure 7. The type I IFN response associated with *PSMD11* variants depends on PKR in affected individuals T cells

(A) IFN scores for subjects 1, 4, 6, and 7 as well as both parents of subject 6 and 6 unrelated healthy donor (HD) controls were calculated as the median of the relative quantifications of the 7 ISGs over a single calibrator control. Shown are the IFN scores of each sample (left) and the sample groups, namely healthy donors (HDs) and subjects carrying *PSMD11* variants, as indicated. Statistical significance was assessed by unpaired t test where * indicates $p < 0.05$.

(B) T cells from subjects 6, 7, and 8 were subjected to a 6-h treatment with DMSO (vehicle), 4μ8C (100 μM), C16 (500 nM), or H-151 (2 μM) small-molecule inhibitors before RNA extraction and RT-qPCR for expression analysis of *IFIT1*, *IFI27*, *IFI44*, *IFI44L*, *ISG15*, *MX1*, and *RSAD2*. Transcript expression was normalized to *GAPDH* and data are presented as the fold-change median values of the 7 ISGs relative to DMSO (gridline) for each subject in each treatment. Columns indicate the fold-change mean values ± SEM of the subject group ($n = 3$) for each treatment. Statistical significance was assessed by ratio paired t test where *** indicates $p < 0.001$.

(Figure S4). This unambiguously classifies the identified *PSMD11* variants as loss of function. This aligns with the putative role of the PSMD11 subunit in proteasome abundance and assembly rate limitation,[64,65] which explains why highly proteasome-demanding tissues and cell populations, such as embryonic stem cells (ESCs), are enriched with PSMD11 proteins.[64] Of note, unlike the truncating *PSMD11* variants, which undergo NMD resulting in *PSMD11* haploinsufficiency (Figure S3), the missense variants c.788C>T (p.Thr263Ile) and c.914C>T (p.Ala305Val) appeared hypomorphic, as evidenced by their minimal impact on the steady-state expression level of the PSMD11 subunit (Figure 5). This observation suggests that the *PSMD11* compound missense variants employ an alternative mechanism to downregulate 26S proteasome complexes, distinct from haploinsufficiency. Interestingly, our data suggest that changes in the phosphorylation of the PSMD11 subunit may play a role in this process. Indeed, the phosphorylation status of PSMD11, which is thought to regulate proteasome assembly and activity,[46,47] was compromised in all T cells carrying *PSMD11* missense variants, especially the c.788C>T (p.Thr263Ile) variant, inducing significant decline in (p)PSMD11 (Figure 5). This indicates that this specific residue may be a key phosphorylation site. While recent studies identified Ser14 as a major phosphorylation target in the heart,[66] it is possible that PSMD11 may be phosphorylated on different residues in various tissues and/or cell types, including T cells used in our study. Further studies are needed to establish a causal relationship between reduced (p)PSMD11 levels and decreased abundance of 26S proteasome complexes in subjects with NDD.

While we did not establish a clear genotype-phenotype correlation, our experiments highlighted a milder pathogenicity of the c.788C>T (p.Thr263Ile) and c.914C>T (p.Ala305Val) heterozygous variants. Notably, despite their significant negative *in vitro* effect on proteasome dysfunction (Figure 4A), these 2 *PSMD11* missense variants did not result in clinical manifestations in heterozygous parents. In addition, although their (p)PSMD11 expression level was reduced compared to healthy donor controls, it remained higher than in their daughter (Figure 5). In the same way, in unrelated families 1 and 2, the variant c.268C>T (p.Arg90*) was inherited from fathers who exhibited mild developmental delay (Table S1). By contrast, the severe phenotype in subjects 1 and 2 can be attributed to a second event involving different genes (*PSMC5* and *BBS9*, respectively). These observations suggest that *PSMD11* pathogenic variants may be more common in adult populations with moderate cognitive, psychiatric, or mood disorders than initially thought, and subsequently the presence of individuals with borderline/mild intellectual disability and a *PSMD11* pathogenic variant in public databases is not excluded. These phenotypic elements and the cautiousness in filtering candidate variants were taken into account in our work, leading us to gather

and explore variants found in the GnomAD database in rare occurrences (Table S2).

Remarkably, our transcriptomic studies also revealed that histone genes were consistently downregulated in 2 subjects compared to 3 unrelated healthy individuals. This expression pattern seems specific to *PSMD11* dysfunction, as it was not observed in NDD subjects with *PSMC3* or *PSMC5* variants.[29,67] The feature is intriguing considering that PSMC3, PSMC5, and PSMD11 subunits belong to the same 19S RP and supports the view that PSMD11 may exert proteasome-independent functions, as previously suggested.[68]

Finally, our study also unveils some of the neuronal consequences of *PSMD11* variants. In line with *Rpt5* depletion,[29] gene silencing of *Rpn6* impaired reversal learning in *Drosophila* (Figure 3C), indicating that proteasome loss of function reduces cognitive flexibility. The molecular mechanisms remain unclear but may reflect perturbations in neurite asymmetrical body remodeling, a process reliant on the UPS and critical for sensory perception, as previously proposed.[45] It may also involve hindered breakdown of key synaptic transmission regulators like Arc/Arg3.1 (Arc).[69] As a pivotal player of synaptic plasticity, the accumulation of Arc could indeed perturb glutamatergic synapses, thereby impacting cognitive processes. Alternatively, variants in 19S RP subunit genes like *PSMD11* might impact cognitive flexibility through a mechanism independent of proteasome proteolytic activities. It was indeed recently postulated that 19S RP could function in synapses as independent complexes not needing any binding to 20S CP, regulating the trafficking of AMPA receptors through their intrinsic de-ubiquitinating activity.[70] Eventually, *PSMD11* variants might disrupt interactions between 26S proteasomes and certain proteins responsible for their intracellular distribution within neurons. Such proteins include, for instance, PI31, which binds to 20S complexes,[71] and ECM29, which binds to 26S proteasomes.[72] These 2 proteins help 26S complexes to reach synapses[73] or endosomal components[74] via microtubules. Compromising these interactions would consequently affect the distribution and function of 26S proteasomes in neurons.

Altogether, our work expands the group of neurodevelopmental proteasomopathies and highlights their consistent biological defects characterized by proteasome dysfunction, constitutively activated ISR, and persistent type I IFN signaling. Our work also expands the phenotypic spectrum of proteasome-related NDDs, unveiling a potential regulation of metabolism in addition to neurological involvement, in subjects with a milder cognitive impairment. In this regard, it would be particularly valuable to investigate whether *PSMD11* operates within the context of the proteasome or functions independently in the development of dysregulated metabolism and obesity. Future research will be essential in identifying molecular levers of such pathophysiological processes in more affected subjects, determining the contribution of these biomarkers to disease pathogenesis, with the aim of identifying potential molecular targets in neurodevelopmental proteasomopathies and other more common disease entities.

Data and code availability

All raw data presented in this paper are available to qualified researchers upon request. *Drosophila* lines can be obtained from the Bloomington *Drosophila* Stock Center. Datasets from transcriptomics analysis (NanoString) haven been deposited to the GEO repository with the accession number GSE262901.

Supplemental information

Supplemental information can be found online at https://doi.org/10.1016/j.ajhg.2024.05.016.

Acknowledgments

F.E. acknowledges the I-SITE NExT Junior Talent Chair. S.K. received research grants from the Agence Nationale de la Recherche (ANR) for projects ANR-21-CE17-0005 (UPS-NDDecipher) and ANR-22-RAR4-0001-01 (UPS-NDDiag), as well as support from la Région des Pays de la Loire for project TN_2021_AAP_UPS-NDDECIPHER_INSERM_154550. EJP RD funding was received from the European Union's Horizon 2020 research and innovation program under grant agreement N°825575. S.B. received financial support from the University Hospital Center (CHU) of Nantes for the BioTND-UPS biobank (PROG/09/72-03), and S.B., S.K., and F.E. received funding from Mutuelles AXA for project TND-UPS. E.K. was funded by the German Research Foundation (RTG PRO 2719) and COST Action ProteoCure CA20113. J.E.P., J.R.L., D.P., and D.G.C. received support from various sources including the US National Institutes of Health, Rett Syndrome Research Trust, International Rett Syndrome Foundation, Doris Duke Charitable Foundation, Blue Bird Circle Foundation, and the Muscular Dystrophy Association. One author is part of the European Reference Network on Rare Congenital Malformations and Rare Intellectual Disability ERN-ITHACA. The authors thank Robert Beyer and Anne Brandenburg for their technical assistance.

Author contributions

W.D., S.B., S.K., E.K., and F.E. conceived the study and designed the experiments. W.D. and S.K. supervised subject enrollment. Genomic data analysis was supervised by T.B., B.C., W.D., S.B., and S.K. C.R. and F.V.B. designed, conducted, and analyzed the *Drosophila* behavioral studies. J.J.P., V.V., and F.E. performed and analyzed the functional studies on biological samples. Clinical data were collected and analyzed by W.D., S. Mercier, B.I., S.B., and S.K. Gene expression analysis by NanoString was made by M.S.-T., F.E., and E.K. W.D., V.V., L.R., S. Möller, M.W., B.T., L.P., A.C., A.K., J.dM., J.V., M.N., L.K., M.M.v.H., L.Z., T.S., H.K., R.F., P.S., K.S., B.J., S.Z., A.P.A.S., N.N., C.M.S., C.G., J.R.M., S.I., D.P., D.G.C., J.E.P., K.M., and J.R.L. provided critical material and/or data to carry out the research. Funding acquisition was secured by S.K., S.B., E.K., and F.E.

Declaration of interests

A.C. and K.M. are employees of GeneDx, LLC. J.R.L. has stock in 23andMe and is a paid consultant for Genome International.

Received: November 1, 2023
Accepted: May 16, 2024
Published: June 11, 2024

Web resources

Genome Aggregation Database (GnomAD), accessed September 2023.
Genotype-Tissue Expression (GTEx) Portal: GTEx Analysis Release V8 (dbGaP Accession phs000424.v8.p2), accessed September 2023.
The Human Protein Atlas database: proteinatlas.org, accessed September 2023.

References

1. Schmid, H.P., Akhayat, O., Martins De Sa, C., Puvion, F., Koehler, K., and Scherrer, K. (1984). The prosome: an ubiquitous morphologically distinct RNP particle associated with repressed mRNPs and containing specific ScRNA and a characteristic set of proteins. EMBO J. *3*, 29–34. https://doi.org/10.1002/j.1460-2075.1984.tb01757.x.
2. Arrigo, A.P., Tanaka, K., Goldberg, A.L., and Welch, W.J. (1988). Identity of the 19S "prosome" particle with the large multifunctional protease complex of mammalian cells (the proteasome). Nature *331*, 192–194. https://doi.org/10.1038/331192a0.
3. Falkenburg, P.E., Haass, C., Kloetzel, P.M., Niedel, B., Kopp, F., Kuehn, L., and Dahlmann, B. (1988). Drosophila small cytoplasmic 19S ribonucleoprotein is homologous to the rat multicatalytic proteinase. Nature *331*, 190–192. https://doi.org/10.1038/331190a0.
4. Collins, G.A., and Goldberg, A.L. (2017). The Logic of the 26S Proteasome. Cell *169*, 792–806. https://doi.org/10.1016/j.cell.2017.04.023.
5. Ebstein, F., Kloetzel, P.-M., Krüger, E., and Seifert, U. (2012). Emerging roles of immunoproteasomes beyond MHC class i antigen processing. Cell. Mol. Life Sci. *69*, 2543–2558. https://doi.org/10.1007/s00018-012-0938-0.
6. Tanaka, K. (2009). The proteasome: Overview of structure and functions. Proc. Jpn. Acad. Ser. B Phys. Biol. Sci. *85*, 12–36. https://doi.org/10.2183/pjab.85.12.
7. Gallastegui, N., and Groll, M. (2010). The 26S proteasome: assembly and function of a destructive machine. Trends Biochem. Sci. *35*, 634–642. https://doi.org/10.1016/j.tibs.2010.05.005.
8. Bard, J.A.M., Goodall, E.A., Greene, E.R., Jonsson, E., Dong, K.C., and Martin, A. (2018). Structure and Function of the 26S Proteasome. Annu. Rev. Biochem. *87*, 697–724. https://doi.org/10.1146/annurev-biochem-062917-011931.
9. Greene, E.R., Dong, K.C., and Martin, A. (2020). Understanding the 26S proteasome molecular machine from a structural and conformational dynamics perspective. Curr. Opin. Struct. Biol. *61*, 33–41. https://doi.org/10.1016/j.sbi.2019.10.004.
10. Goetzke, C.C., Ebstein, F., and Kallinich, T. (2021). Role of Proteasomes in Inflammation. J. Clin. Med. *10*, 1783. https://doi.org/10.3390/JCM10081783.
11. Davidson, K., and Pickering, A.M. (2023). The proteasome: A key modulator of nervous system function, brain aging, and neurodegenerative disease. Front. Cell Dev. Biol. *11*, 1124907. https://doi.org/10.3389/fcell.2023.1124907.
12. Ross, C.A., and Poirier, M.A. (2004). Protein aggregation and neurodegenerative disease. Nat. Med. *10*, S10–S17. https://doi.org/10.1038/nm1066.
13. Papendorf, J.J., Krüger, E., and Ebstein, F. (2022). Proteostasis Perturbations and Their Roles in Causing Sterile Inflammation and Autoinflammatory Diseases. Cells *11*, 1422. https://doi.org/10.3390/CELLS11091422.
14. Liu, Y., Ramot, Y., Torrelo, A., Paller, A.S., Si, N., Babay, S., Kim, P.W., Sheikh, A., Lee, C.C.R., Chen, Y., et al. (2012). Mutations in proteasome subunit β type 8 cause chronic atypical neutrophilic dermatosis with lipodystrophy and elevated temperature with evidence of genetic and phenotypic heterogeneity. Arthritis Rheum. *64*, 895–907. https://doi.org/10.1002/art.33368.
15. Brehm, A., Liu, Y., Sheikh, A., Marrero, B., Omoyinmi, E., Zhou, Q., Montealegre, G., Biancotto, A., Reinhardt, A., Almeida de Jesus, A., et al. (2015). Additive loss-of-function proteasome subunit mutations in CANDLE/PRAAS patients promote type I IFN production. J. Clin. Invest. *125*, 4196–4211. https://doi.org/10.1172/JCI81260.
16. Yamazaki-Nakashimada, M.A., Santos-Chávez, E.E., De Jesus, A.A., Rivas-Larrauri, F., Guzmán-Martínez, M.N., Goldbach-Mansky, R., Espinosa-Padilla, S., Sáez-De-Ocariz, M.M., Orozco-Covarrubias, L., and Blancas-Galicia, L. (2019). Systemic autoimmunity in a patient with CANDLE syndrome. J Investig. Allergol. Clin. Immunol. *29*, 75. https://doi.org/10.18176/jiaci.0338.
17. Almeida de Jesus, A., and Goldbach-Mansky, R. (2013). Monogenic autoinflammatory diseases: concept and clinical manifestations. Clin. Immunol. *147*, 155–174. https://doi.org/10.1016/J.CLIM.2013.03.016.
18. Poli, M.C., Ebstein, F., Nicholas, S.K., de Guzman, M.M., Forbes, L.R., Chinn, I.K., Mace, E.M., Vogel, T.P., Carisey, A.F., Benavides, F., et al. (2018). Heterozygous Truncating Variants in POMP Escape Nonsense-Mediated Decay and Cause a Unique Immune Dysregulatory Syndrome. Am. J. Hum. Genet. *102*, 1126–1142. https://doi.org/10.1016/J.AJHG.2018.04.010.
19. Sarrabay, G., Méchin, D., Salhi, A., Boursier, G., Rittore, C., Crow, Y., Rice, G., Tran, T.A., Cezar, R., Duffy, D., et al. (2020). PSMB10, the last immunoproteasome gene missing for PRAAS. J. Allergy Clin. Immunol. *145*, 1015–1017.e6. https://doi.org/10.1016/J.JACI.2019.11.024.
20. Papendorf, J.J., Ebstein, F., Alehashemi, S., Piotto, D.G.P., Kozlova, A., Terreri, M.T., Shcherbina, A., Rastegar, A., Rodrigues, M., Pereira, R., et al. (2023). Identification of eight novel proteasome variants in five unrelated cases of proteasome-associated autoinflammatory syndromes (PRAAS). Front. Immunol. *14*, 1190104. https://doi.org/10.3389/fimmu.2023.1190104.
21. Kitamura, A., Maekawa, Y., Uehara, H., Izumi, K., Kawachi, I., Nishizawa, M., Toyoshima, Y., Takahashi, H., Standley, D.M., Tanaka, K., et al. (2011). A mutation in the immunoproteasome subunit PSMB8 causes autoinflammation and lipodystrophy in humans. J. Clin. Invest. *121*, 4150–4160. https://doi.org/10.1172/JCI58414.
22. Agarwal, A.K., Xing, C., Demartino, G.N., Mizrachi, D., Hernandez, M.D., Sousa, A.B., Martínez De Villarreal, L., Dos Santos, H.G., and Garg, A. (2010). PSMB8 Encoding the β5i

Proteasome Subunit Is Mutated in Joint Contractures, Muscle Atrophy, Microcytic Anemia, and Panniculitis-Induced Lipodystrophy Syndrome. Am. J. Hum. Genet. *87*, 866–872. https://doi.org/10.1016/J.AJHG.2010.10.031.

23. Arima, K., Kinoshita, A., Mishima, H., Kanazawa, N., Kaneko, T., Mizushima, T., Ichinose, K., Nakamura, H., Tsujino, A., Kawakami, A., et al. (2011). Proteasome assembly defect due to a proteasome subunit beta type 8 (PSMB8) mutation causes the autoinflammatory disorder, Nakajo-Nishimura syndrome. Proc. Natl. Acad. Sci. USA. *108*, 14914–14919. https://doi.org/10.1073/PNAS.1106015108.
24. Küry, S., Besnard, T., Ebstein, F., Khan, T.N., Gambin, T., Douglas, J., Bacino, C.A., Sanders, S.J., Lehmann, A., Latypova, X., et al. (2017). De Novo Disruption of the Proteasome Regulatory Subunit PSMD12 Causes a Syndromic Neurodevelopmental Disorder. Am. J. Hum. Genet. *100*, 352–363. https://doi.org/10.1016/j.ajhg.2017.01.003.
25. Khalil, R., Kenny, C., Hill, R.S., Mochida, G.H., Nasir, R., Partlow, J.N., Barry, B.J., Al-Saffar, M., Egan, C., Stevens, C.R., et al. (2018). PSMD12 haploinsufficiency in a neurodevelopmental disorder with autistic features. Am. J. Med. Genet. B Neuropsychiatr. Genet. *177*, 736–745. https://doi.org/10.1002/ajmg.b.32688.
26. Isidor, B., Ebstein, F., Hurst, A., Vincent, M., Bader, I., Rudy, N.L., Cogne, B., Mayr, J., Brehm, A., Bupp, C., et al. (2022). Stankiewicz-Isidor syndrome: expanding the clinical and molecular phenotype. Genet. Med. *24*, 179–191. https://doi.org/10.1016/J.GIM.2021.09.005.
27. Aharoni, S., Proskorovski-Ohayon, R., Krishnan, R.K., Yogev, Y., Wormser, O., Hadar, N., Bakhrat, A., Alshafee, I., Gombosh, M., Agam, N., et al. (2022). PSMC1 variant causes a novel neurological syndrome. Clin. Genet. *102*, 324–332. https://doi.org/10.1111/cge.14195.
28. Kröll-Hermi, A., Ebstein, F., Stoetzel, C., Geoffroy, V., Schaefer, E., Scheidecker, S., Bär, S., Takamiya, M., Kawakami, K., Zieba, B.A., et al. (2020). Proteasome subunit PSMC3 variants cause neurosensory syndrome combining deafness and cataract due to proteotoxic stress. EMBO Mol. Med. *12*, e11861. https://doi.org/10.15252/emmm.201911861.
29. Ebstein, F., Küry, S., Most, V., Rosenfelt, C., Scott-Boyer, M.-P., van Woerden, G.M., Besnard, T., Papendorf, J.J., Studencka-Turski, M., Wang, T., et al. (2023). PSMC3 proteasome subunit variants are associated with neurodevelopmental delay and type I interferon production. Sci. Transl. Med. *15*, eabo3189. https://doi.org/10.1126/scitranslmed.abo3189.
30. Ansar, M., Ebstein, F., Özkoç, H., Paracha, S.A., Iwaszkiewicz, J., Gesemann, M., Zoete, V., Ranza, E., Santoni, F.A., Sarwar, M.T., et al. (2020). Biallelic variants in PSMB1 encoding the proteasome subunit β6 cause impairment of proteasome function, microcephaly, intellectual disability, developmental delay and short stature. Hum. Mol. Genet. *29*, 1132–1143. https://doi.org/10.1093/HMG/DDAA032.
31. Ebstein, F., Poli Harlowe, M.C., Studencka-Turski, M., and Krüger, E. (2019). Contribution of the Unfolded Protein Response (UPR) to the Pathogenesis of Proteasome-Associated Autoinflammatory Syndromes (PRAAS). Front. Immunol. *10*, 2756. https://doi.org/10.3389/fimmu.2019.02756.
32. Ebstein, F., Küry, S., Papendorf, J.J., and Krüger, E. (2021). Neurodevelopmental Disorders (NDD) Caused by Genomic Alterations of the Ubiquitin-Proteasome System (UPS): the Possible Contribution of Immune Dysregulation to Disease Pathogenesis. Front. Mol. Neurosci. *14*, 733012. https://doi.org/10.3389/fnmol.2021.733012.
33. Cuinat, S., Bézieau, S., Deb, W., Mercier, S., Vignard, V., Isidor, B., Küry, S., and Ebstein, F. (2023). Understanding neurodevelopmental proteasomopathies as new rare disease entities: A review of current concepts, molecular biomarkers, and perspectives. Genes Dis. 101130. https://doi.org/10.1016/j.gendis.2023.101130.
34. Richards, S., Aziz, N., Bale, S., Bick, D., Das, S., Gastier-Foster, J., Grody, W.W., Hegde, M., Lyon, E., Spector, E., et al. (2015). Standards and guidelines for the interpretation of sequence variants: a joint consensus recommendation of the American College of Medical Genetics and Genomics and the Association for Molecular Pathology. Genet. Med. *17*, 405–424. https://doi.org/10.1038/gim.2015.30.
35. Sobreira, N., Schiettecatte, F., Valle, D., and Hamosh, A. (2015). GeneMatcher: a matching tool for connecting investigators with an interest in the same gene. Hum. Mutat. *36*, 928–930. https://doi.org/10.1002/HUMU.22844.
36. Baux, D., Van Goethem, C., Ardouin, O., Guignard, T., Bergougnoux, A., Koenig, M., and Roux, A.F. (2021). MobiDetails: online DNA variants interpretation. Eur. J. Hum. Genet. *29*, 356–360. https://doi.org/10.1038/s41431-020-00755-z.
37. Backenroth, D., Homsy, J., Murillo, L.R., Glessner, J., Lin, E., Brueckner, M., Lifton, R., Goldmuntz, E., Chung, W.K., and Shen, Y. (2014). CANOES: detecting rare copy number variants from whole exome sequencing data. Nucleic Acids Res. *42*, e97. https://doi.org/10.1093/nar/gku345.
38. Tully, T., and Quinn, W.G. (1985). Classical conditioning and retention in normal and mutant Drosophila melanogaster. J. Comp. Physiol. *157*, 263–277. https://doi.org/10.1007/BF01350033.
39. Tully, T., Boyton, S., Brandes, C., Dura, J.M., Mihalek, R., Preat, T., and Villella, A. (1990). Genetic dissection of memory formation in Drosophila melanogaster. In Cold Spring Harbor Symposia on Quantitative Biology. https://doi.org/10.1101/SQB.1990.055.01.022.
40. Fonteneau, J.F., Larsson, M., Somersan, S., Sanders, C., Münz, C., Kwok, W.W., Bhardwaj, N., and Jotereau, F. (2001). Generation of high quantities of viral and tumor-specific human CD4+ and CD8+ T-cell clones using peptide pulsed mature dendritic cells. J. Immunol. Methods *258*, 111–126. https://doi.org/10.1016/S0022-1759(01)00477-X.
41. Lintas, C., Sacco, R., Tabolacci, C., Brogna, C., Canali, M., Picinelli, C., Tomaiuolo, P., Castronovo, P., Baccarin, M., and Persico, A.M. (2019). An interstitial 17q11.2 de novo deletion involving the CDK5R1 gene in a high-functioning autistic patient. Mol. Syndromol. *9*, 247–252. https://doi.org/10.1159/000491802.
42. Wang, X., Cimermancic, P., Yu, C., Schweitzer, A., Chopra, N., Engel, J.L., Greenberg, C., Huszagh, A.S., Beck, F., Sakata, E., et al. (2017). Molecular Details Underlying Dynamic Structures and Regulation of the Human 26S Proteasome. Mol. Cell. Proteomics *16*, 840–854. https://doi.org/10.1074/MCP.M116.065326.
43. Pathare, G.R., Nagy, I., Bohn, S., Unverdorben, P., Hubert, A., Körner, R., Nickell, S., Lasker, K., Sali, A., Tamura, T., et al. (2012). The proteasomal subunit Rpn6 is a molecular clamp holding the core and regulatory subcomplexes together. Proc. Natl. Acad. Sci. USA *109*, 149–154. https://doi.org/10.1073/pnas.1117648108.

44. Andreutti-Zaugg, C., Scott, R.J., and Iggo, R. (1997). Inhibition of nonsense-mediated messenger RNA decay in clinical samples facilitates detection of human MSH2 mutations with an in vivo fusion protein assay and conventional techniques. Cancer Res. *57*, 3288–3293.
45. Sakamura, S., Hsu, F.-Y., Tsujita, A., Abubaker, M.B., Chiang, A.-S., and Matsuno, K. (2023). Ecdysone signaling determines lateral polarity and remodels neurites to form Drosophila's left-right brain asymmetry. Cell Rep. *42*, 112337. https://doi.org/10.1016/j.celrep.2023.112337.
46. Lokireddy, S., Kukushkin, N.V., and Goldberg, A.L. (2015). cAMP-induced phosphorylation of 26S proteasomes on Rpn6/PSMD11 enhances their activity and the degradation of misfolded proteins. Proc. Natl. Acad. Sci. USA *112*, E7176–E7185. https://doi.org/10.1073/pnas.1522332112.
47. VerPlank, J.J.S., Lokireddy, S., Zhao, J., and Goldberg, A.L. (2019). 26S Proteasomes are rapidly activated by diverse hormones and physiological states that raise cAMP and cause Rpn6 phosphorylation. Proc. Natl. Acad. Sci. USA *116*, 4228–4237. https://doi.org/10.1073/pnas.1809254116.
48. Rice, G.I., Melki, I., Frémond, M.L., Briggs, T.A., Rodero, M.P., Kitabayashi, N., Oojageer, A., Bader-Meunier, B., Belot, A., Bodemer, C., et al. (2017). Assessment of Type I Interferon Signaling in Pediatric Inflammatory Disease. J. Clin. Immunol. *37*, 123–132. https://doi.org/10.1007/S10875-016-0359-1.
49. Davidson, S., Yu, C.H., Steiner, A., Ebstein, F., Baker, P.J., Jarur-Chamy, V., Hrovat Schaale, K., Laohamonthonkul, P., Kong, K., Calleja, D.J., et al. (2022). Protein kinase R is an innate immune sensor of proteotoxic stress via accumulation of cytoplasmic IL-24. Sci. Immunol. *7*, eabi6763. https://doi.org/10.1126/SCIIMMUNOL.ABI6763.
50. Sulkshane, P., Duek, I., Ram, J., Thakur, A., Reis, N., Ziv, T., and Glickman, M.H. (2020). Inhibition of proteasome reveals basal mitochondrial ubiquitination. J. Proteomics *229*, 103949. https://doi.org/10.1016/j.jprot.2020.103949.
51. Parenti, I., Rabaneda, L.G., Schoen, H., and Novarino, G. (2020). Neurodevelopmental Disorders: From Genetics to Functional Pathways. Trends Neurosci. *43*, 608–621. https://doi.org/10.1016/j.tins.2020.05.004.
52. Spedicati, B., Morgan, A., Pianigiani, G., Musante, L., Rubinato, E., Santin, A., Nardone, G.G., Faletra, F., and Girotto, G. (2022). Challenging Occam's Razor: Dual Molecular Diagnoses Explain Entangled Clinical Pictures. Genes *13*, 2023. https://doi.org/10.3390/genes13112023.
53. Posey, J.E., Harel, T., Liu, P., Rosenfeld, J.A., James, R.A., Coban Akdemir, Z.H., Walkiewicz, M., Bi, W., Xiao, R., Ding, Y., et al. (2017). Resolution of Disease Phenotypes Resulting from Multilocus Genomic Variation. N. Engl. J. Med. *376*, 21–31. https://doi.org/10.1056/NEJMoa1516767.
54. Kim, H., Sanchez, G.A.M., and Goldbach-Mansky, R. (2016). Insights from Mendelian Interferonopathies: Comparison of CANDLE, SAVI with AGS, Monogenic Lupus. J. Mol. Med. *94*, 1111–1127. https://doi.org/10.1007/s00109-016-1465-5.
55. Miyake, M., Zhang, J., Yasue, A., Hisanaga, S., Tsugawa, K., Sakaue, H., Oyadomari, M., Kiyonari, H., and Oyadomari, S. (2021). Integrated stress response regulates GDF15 secretion from adipocytes, preferentially suppresses appetite for a high-fat diet and improves obesity. iScience *24*, 103448. https://doi.org/10.1016/j.isci.2021.103448.
56. Nakamura, T., Kunz, R.C., Zhang, C., Kimura, T., Yuan, C.L., Baccaro, B., Namiki, Y., Gygi, S.P., and Hotamisligil, G.S. (2015). A critical role for PKR complexes with TRBP in Immunometabolic regulation and eIF2α phosphorylation in obesity. Cell Rep. *11*, 295–307. https://doi.org/10.1016/j.celrep.2015.03.021.
57. Ghazarian, M., Revelo, X.S., Nøhr, M.K., Luck, H., Zeng, K., Lei, H., Tsai, S., Schroer, S.A., Park, Y.J., Chng, M.H.Y., et al. (2017). Type I Interferon Responses Drive Intrahepatic T cells to Promote Metabolic Syndrome. Sci Immunol *2*, eaai7616. https://doi.org/10.1126/sciimmunol.aai7616.
58. Xu, X., Krumm, C., So, J.-S., Bare, C.J., Holman, C., Gromada, J., Cohen, D.E., and Lee, A.-H. (2018). Preemptive Activation of the Integrated Stress Response Protects Mice From Diet-Induced Obesity and Insulin Resistance by Fibroblast Growth Factor 21 Induction. Hepatology *68*, 2167–2181. https://doi.org/10.1002/hep.30060.
59. Huang, L.-Y., Chiu, C.-J., Hsing, C.-H., and Hsu, Y.-H. (2022). Interferon Family Cytokines in Obesity and Insulin Sensitivity. Cells *11*, 4041. https://doi.org/10.3390/cells11244041.
60. Chan, C.C., Damen, M.S.M.A., Moreno-Fernandez, M.E., Stankiewicz, T.E., Cappelletti, M., Alarcon, P.C., Oates, J.R., Doll, J.R., Mukherjee, R., Chen, X., et al. (2020). Type I interferon sensing unlocks dormant adipocyte inflammatory potential. Nat. Commun. *11*, 2745. https://doi.org/10.1038/s41467-020-16571-4.
61. Yuan, J., Yu, Z., Gao, J., Luo, K., Shen, X., Cui, B., and Lu, Z. (2022). Inhibition of GCN2 alleviates hepatic steatosis and oxidative stress in obese mice: Involvement of NRF2 regulation. Redox Biol. *49*, 102224. https://doi.org/10.1016/j.redox.2021.102224.
62. Liu, S., Yuan, J., Yue, W., Bi, Y., Shen, X., Gao, J., Xu, X., and Lu, Z. (2018). GCN2 deficiency protects against high fat diet induced hepatic steatosis and insulin resistance in mice. Biochim. Biophys. Acta, Mol. Basis Dis. *1864*, 3257–3267. https://doi.org/10.1016/j.bbadis.2018.07.012.
63. de Jesus, A.A., Brehm, A., VanTries, R., Pillet, P., Parentelli, A.S., Montealegre Sanchez, G.A., Deng, Z., Paut, I.K., Goldbach-Mansky, R., and Krüger, E. (2019). Novel Proteasome Assembly Chaperone mutations in PSMG2/PAC2, cause the autoinflammatory interferonopathy, CANDLE/PRAAS4. J. Allergy Clin. Immunol. *143*, 1939–1943.e8. https://doi.org/10.1016/J.JACI.2018.12.1012.
64. Vilchez, D., Boyer, L., Morantte, I., Lutz, M., Merkwirth, C., Joyce, D., Spencer, B., Page, L., Masliah, E., Berggren, W.T., et al. (2012). Increased proteasome activity in human embryonic stem cells is regulated by PSMD11. Nature *489*, 304–308. https://doi.org/10.1038/nature11468.
65. Heitmeier, T., Sydykov, A., Lukas, C., Vroom, C., Korfei, M., Petrovic, A., Klingel, K., Günther, A., Eickelberg, O., Weissmann, N., et al. (2020). Altered proteasome function in right ventricular hypertrophy. Cardiovasc. Res. *116*, 406–415. https://doi.org/10.1093/cvr/cvz103.
66. Yang, L., Parajuli, N., Wu, P., Liu, J., and Wang, X. (2023). Ser14-RPN6 Phosphorylation Mediates the Activation of 26S Proteasomes by cAMP and Protects against Cardiac Proteotoxic Stress in Mice. Preprint at bioRxiv. https://doi.org/10.1101/2023.04.05.535705.
67. Küry, S., Stanton, J.E., van Woerden, G., Hsieh, T.-C., Rosenfelt, C., Scott-Boyer, M.P., Most, V., Wang, T., Papendorf, J.J., de Konink, C., et al. (2024). Unveiling the crucial neuronal role of the proteasomal ATPase subunit gene PSMC5 in neurodevelopmental proteasomopathies. Preprint at medRxiv. https://doi.org/10.1101/2024.01.13.24301174.

68. Cal-Kayitmazbatir, S., Francey, L.J., Lee, Y., Liu, A.C., and Hogenesch, J.B. (2023). PSMD11 modulates circadian clock function through PER and CRY nuclear translocation. PLoS One *18*, e0283463. https://doi.org/10.1371/journal.pone.0283463.
69. Wall, M.J., Collins, D.R., Chery, S.L., Allen, Z.D., Pastuzyn, E.D., George, A.J., Nikolova, V.D., Moy, S.S., Philpot, B.D., Shepherd, J.D., et al. (2018). The Temporal Dynamics of Arc Expression Regulate Cognitive Flexibility. Neuron *98*, 1124–1132.e7. https://doi.org/10.1016/j.neuron.2018.05.012.
70. Sun, C., Desch, K., Nassim-Assir, B., Giandomenico, S.L., Nemcova, P., Langer, J.D., and Schuman, E.M. (2023). An abundance of free regulatory (19S) proteasome particles regulates neuronal synapses. Science *380*, eadf2018. https://doi.org/10.1126/science.adf2018.
71. Hsu, H.-C., Wang, J., Kjellgren, A., Li, H., and DeMartino, G.N. (2023). High-resolution structure of mammalian PI31-20S proteasome complex reveals mechanism of proteasome inhibition. J. Biol. Chem. *299*, 104862. https://doi.org/10.1016/j.jbc.2023.104862.
72. Gorbea, C., Goellner, G.M., Teter, K., Holmes, R.K., and Rechsteiner, M. (2004). Characterization of mammalian Ecm29, a 26 S proteasome-associated protein that localizes to the nucleus and membrane vesicles. J. Biol. Chem. *279*, 54849–54861. https://doi.org/10.1074/jbc.M410444200.
73. Liu, K., Jones, S., Minis, A., Rodriguez, J., Molina, H., and Steller, H. (2019). PI31 Is an Adaptor Protein for Proteasome Transport in Axons and Required for Synaptic Development. Dev. Cell *50*, 509–524.e10. https://doi.org/10.1016/j.devcel.2019.06.009.
74. Gorbea, C., Pratt, G., Ustrell, V., Bell, R., Sahasrabudhe, S., Hughes, R.E., and Rechsteiner, M. (2010). A protein interaction network for Ecm29 links the 26 S proteasome to molecular motors and endosomal components. J. Biol. Chem. *285*, 31616–31633. https://doi.org/10.1074/jbc.M110.154120.